Applied Geochemistry 25 (2010) 1431–1452

Contents lists available at ScienceDirect

Applied Geochemistry

journal homepage: www.elsevier.com/locate/apgeochem

Aquifer geochemistry at potential aquifer storage and recovery sites in coastal plain aquifers in the New York city area, USA

Craig J. Brown [a,*], Paul E. Misut [b]

[a] US Geological Survey, 101 Pitkin Street, East Hartford, CT 06108, USA
[b] US Geological Survey, 245 Route 112, Coram, NY 11727, USA

ARTICLE INFO

Article history:
Received 2 January 2010
Accepted 4 July 2010
Available online 8 July 2010
Editorial handling by P.B. McMahon

ABSTRACT

The effects of injecting oxic water from the New York city (NYC) drinking-water supply and distribution system into a nearby anoxic coastal plain aquifer for later recovery during periods of water shortage (aquifer storage and recovery, or ASR) were simulated by a 3-dimensional, reactive-solute transport model. The Cretaceous aquifer system in the NYC area of New York and New Jersey, USA contains pyrite, goethite, locally occurring siderite, lignite, and locally varying amounts of dissolved Fe and salinity. Sediment from cores drilled on Staten Island and western Long Island had high extractable concentrations of Fe, Mn, and acid volatile sulfides (AVS) plus chromium-reducible sulfides (CRS) and low concentrations of As, Pb, Cd, Cr, Cu and U. Similarly, water samples from the Lloyd aquifer (Cretaceous) in western Long Island generally contained high concentrations of Fe and Mn and low concentrations of other trace elements such as As, Pb, Cd, Cr, Cu and U, all of which were below US Environmental Protection Agency (USEPA) and NY maximum contaminant levels (MCLs). In such aquifer settings, ASR operations can be complicated by the oxidative dissolution of pyrite, low pH, and high concentrations of dissolved Fe in extracted water.

The simulated injection of buffered, oxic city water into a hypothetical ASR well increased the hydraulic head at the well, displaced the ambient groundwater, and formed a spheroid of injected water with lower concentrations of Fe, Mn and major ions in water surrounding the ASR well, than in ambient water. Both the dissolved O_2 concentrations and the pH of water near the well generally increased in magnitude during the simulated 5-a injection phase. The resultant oxidation of Fe^{2+} and attendant precipitation of goethite during injection provided a substrate for sorption of dissolved Fe during the 8-a extraction phase. The baseline scenario with a low (0.001 M) concentration of pyrite in aquifer sediments, indicated that nearly 190% more water with acceptably low concentrations of dissolved Fe could be extracted than was injected. Scenarios with larger amounts of pyrite in aquifer sediments generally resulted in less goethite precipitation, increased acidity, and increased concentrations of dissolved Fe in extracted water. In these pyritic scenarios, the lower amounts of goethite precipitated and the lower pH during the extraction phase resulted in decreased sorption of Fe^{2+} and a decreased amount of extractable water with acceptably low concentrations of dissolved Fe (5.4×10^{-6} M). A linear decrease in recovery efficiency with respect to dissolved Fe concentrations is caused by pyrite dissolution and the associated depletion of dissolved O_2 (DO) and increase in acidity. Simulations with more than 0.0037 M of pyrite, which is the maximum amount dissolved in the baseline scenario, had just over a 50% recovery efficiency. The precipitation of ferric hydroxide minerals (goethite) at the well screen, and a possible associated decrease in specific capacity of the ASR well, was not apparent during the extraction phase of ASR simulations, but the model does not incorporate the microbial effects and biofouling associated with ferric hydroxide precipitation.

The host groundwater chemistry in calcite-poor Cretaceous aquifers of the NYC area consists of low alkalinity and moderate to low pH. The dissolution of goethite in scenarios with unbuffered injectate indicates that corrosion of the well could occur if the injectate is not buffered. Simulations with buffered injectate resulted in greater precipitation of goethite, and lower concentrations of dissolved Fe, in the extracted water. Dissolved Fe concentrations in extracted water were highest in simulations of aquifers (1) in which pyrite and siderite in the aquifer were in equilibrium, and (2) in coastal areas affected by

* Corresponding author. Fax: +1 860 291 6799.
E-mail address: cjbrown@usgs.gov (C.J. Brown).

0883-2927/$ - see front matter Published by Elsevier Ltd.
doi:10.1016/j.apgeochem.2010.07.001

saltwater intrusion, where high dissolved-cation concentrations provide a greater exchange of Fe^{2+} (FeX_2). Results indicate that ASR in pyrite-bearing, Cretaceous aquifers of the NYC area can be a cost effective way to both store drinking water supplies and significantly reduce ambient concentrations of dissolved Fe.

Published by Elsevier Ltd.

1. Introduction

The injection of water into an aquifer for later recovery when needed, a process known as "aquifer storage and recovery" (ASR), has been used for many years around the world to provide a source of water for future use. The success or failure of ASR depends on the quantity and quality of water that can be recovered, and these in turn are functions of the hydrogeologic, geochemical, and microbiological characteristics of the aquifer. The injectate (water injected into the aquifer) is typically clean, oxic water; theoretically, this water should form a spheroid, although physical heterogeneities such as low permeability zones that are inherent in most aquifers tend to inhibit the recovery and can result in significant dispersion (Vacher et al., 2006; Pavelic et al., 2007). In addition, ASR can trigger several geochemical processes that can affect (1) the water and minerals within the aquifer, and (2) the water that is subsequently extracted. Studies at ASR sites around the world have reported changes in the chemical quality of the recovered water, including increased concentrations of F (Gaus et al., 2002), Fe, Mn, As, Mn, Ni, Co, and other elements (Pyne, 1995; Pavelic and Dillon, 1997; Mirecki, 2004; Brown et al., 2006), and the formation of the disinfection byproducts trihalomethanes (THMs) and haloacetic acids (Katzer and Brothers, 1989; Baqai, 2002). Recovery efficiency refers to the percentage of water volume stored that is subsequently recovered while meeting a target (Pyne, 1995)—in the case of ASR in aquifers with high dissolved Fe, the target is generally the secondary maximum contaminant level (SMCL) for dissolved Fe of 5.4×10^{-6} M. An additional complication can be biofouling of the well, which generally occurs to a far greater extent during extraction than during injection. The development of biofilms in the aquifer matrix or well screen (Pyne, 1995; Mettler et al., 2001) can lead to precipitation of Fe(III) and Mn(IV) oxyhydroxides and thereby inhibit the rate and volume of recovery.

In situ Fe removal, which is operationally similar to ASR, has been used effectively around the world to lower concentrations of dissolved Fe in extracted native groundwater after injection of oxygenated water (Hallberg and Martinell, 1976; Booch and Barovich, 1981; Van Beek, 1980; Rott and Lamberth, 1993; Appelo et al., 1999). The increase in recovery efficiency is attributed to the oxidation of sorbed and exchangeable Fe^{2+} to form Fe oxyhydroxides during injection and to the resulting increase in sorption capacity for Fe^{2+} during extraction and successive ASR cycles (Van Beek and Vaessen, 1979; Appelo et al., 1999). A study of an alluvial aquifer at an in situ Fe removal plant found that the Fe^{2+} generally precipitated as a crystalline ferric oxide that was mostly goethite (FeOOH) (Mettler et al., 2001). In the presence of Fe-sulfide minerals (e.g., FeS_2), the decrease in pH associated with the oxidation of these minerals results in less sorption of Fe^{2+} during extraction than in sulfide-free aquifers (Appelo et al., 1999). In coastal areas, mixture of groundwater with seawater generally results in the exchange of Ca^{2+} and Fe for Na^{+} and a decrease in pH (Appelo and Postma, 1993), which could lead to decreased recovery efficiency with respect to dissolved Fe.

ASR technology is under consideration by the NYC Department of Environmental Protection (NYCDEP) for use during times of drought or water-tunnel repair. The Cretaceous deposits that form several major water-supply aquifers beneath western Long Island and Staten Island (Fig. 1) generally are confined and thick enough to warrant such use. Public-water supply for the New York (NY) counties of Kings, Queens, Manhattan, and Richmond (Staten Island) has been provided mainly by NYC's surface-water-reservoir system in upstate NY since 1971. Prior to dependence on upstate surface water, water supply for these areas included extensive groundwater pumped in Kings and Queens, which resulted in severe water-level declines and saltwater intrusion along the coastline. Over the past several years, substantial leakage through tunnel fractures in upstate NY has been identified and NYCDEP plans to temporarily shut down some tunnels and seal the fractures to prevent the loss of water. Groundwater-modeling studies by the US Geological Survey (USGS) indicate that additional pumping in coastal areas of Long Island and throughout Staten Island would exacerbate saltwater intrusion (Misut and Voss, 2007), but ASR programs could also help alleviate these conditions.

The Lloyd and Magothy aquifers in Staten Island and Long Island can contain a range of concentrations of dissolved Fe and Mn, Fe sulfides and oxides, lignite, and locally occurring siderite, and generally are free of carbonate minerals (Brown et al., 2000a,b; Pearson and Friedman, 1970). These minerals could hamper the efficacy of ASR operations through reactions such as dissolution of Fe-sulfide minerals and the subsequent increase in acidity, ion exchange, the dissolution or precipitation of $Fe(OH)_3$, and the potential mobilization of naturally occurring constituents. This paper examines these processes that are common to the Long Island-NYC area, as well as northern New Jersey (NJ) and other pyrite-bearing coastal plain aquifer systems, based on solid-phase geochemistry, groundwater geochemistry, and reactive solute-transport modeling.

2. Study area

The study area, which encompasses part of the northern Atlantic Coastal Plain including Staten Island and Long Island, NY and part of Monmouth County in northeastern NJ (Fig. 1), is underlain by a sequence of Cretaceous, Pleistocene, and Recent deposits that overlie a southeastward dipping bedrock surface (Figs. 1 and 2; Zapecza, 1989; Soren, 1988; Smolensky et al., 1989; Buxton and Shernoff, 1999). Only the Cretaceous deposits were addressed in this study.

2.1. Hydrogeology

The bedrock surface beneath western Long Island (Kings and Queens Counties, Fig. 1) is overlain by the Cretaceous-age Raritan Formation, which includes the Lloyd basal sand member (the Lloyd aquifer) and an unnamed clay (Raritan confining unit); see sections A–A′ and B–B′ in Fig. 2. The Raritan deposits thicken southeastward and reach a thickness of about 150 m on Staten Island and 250 m in Kings and Queens Counties. The Lloyd sand member consists mainly of nonmarine deltaic deposits of fine to coarse quartzose sand and gravel, with interbeds of silt and clay and clayey sand. The Raritan is overlain by the Matawan Group and Magothy Formation, undifferentiated, which make up the Magothy aquifer, also of Cretaceous age. The Magothy aquifer consists mostly of deltaic quartzose very fine to coarse sand and silty sand with lesser amounts of interbedded clay and silt. The Lloyd and Magothy aquifers contain locally abundant lignite and Fe-sulfide minerals. The depositional environment of Magothy aquifer deposits of Long Island is predominantly transitional-nonmarine, but varies to a transitional-marine depositional environment in some areas near the south shore (Brown et al., 2000b), and may be locally reworked

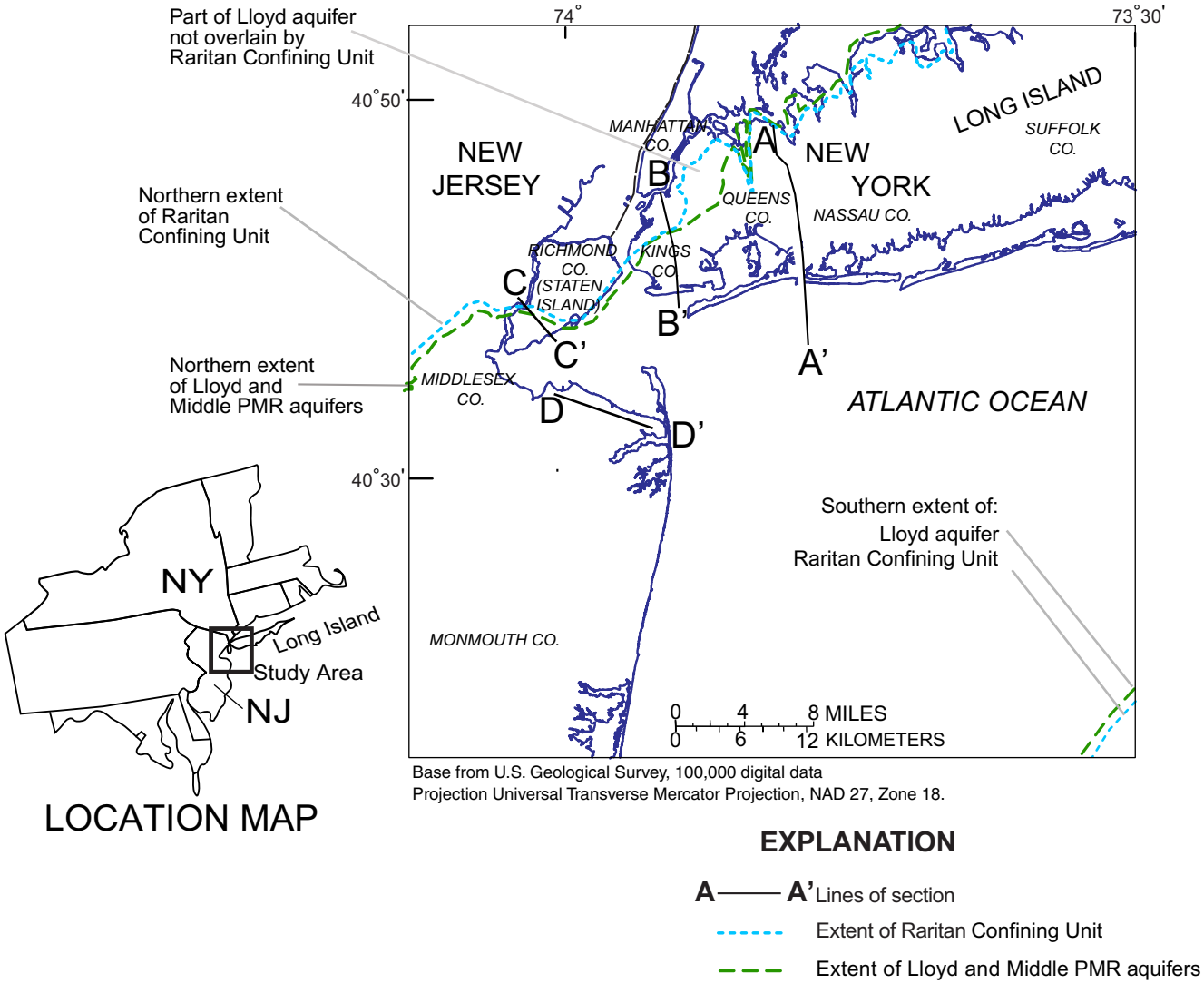

Fig. 1. Pertinent geographic features of the study area in New York city and surrounding areas (sections A–A′, B–B′, C–C′, and D–D′ are depicted in Fig. 2).

with overlying Cretaceous marine sediments of the Monmouth greensand along the south shore of central and eastern Long Island (Smolensky et al., 1989). Along the south shore of western Long Island, the Magothy aquifer is unconformably overlain by the Jameco gravel (Jameco aquifer) of Pleistocene age, which is present in most of Kings and southern Queens County, but not along the lines of the four vertical sections depicted in Fig. 2. The Magothy and Jameco aquifers can be considered as a single aquifer (Jameco–Magothy aquifer) in most of western Long Island because they are hydraulically connected. In the southwestern part of Long Island, the Jameco is unconformably overlain by the Gardiners Clay (an Upper Pleistocene interglacial unit) that extends along much of Long Island's south shore and by glacial deposits that form the upper glacial aquifer of Pleistocene age. Cretaceous deposits north of the Gardiners Clay are unconformably overlain by the upper glacial aquifer (Buxton and Modica, 1992).

The Cretaceous deposits of Staten Island (section C–C′ in Fig. 2) are considered the equivalent of the Raritan Formation, undivided, of Long Island and consist of stratified beds and lenses of clay, silt, and sand, in which lignite and Fe-sulfide minerals are common (Soren, 1988). The Raritan Formation of Long Island differs from New Jersey's Raritan Formation (Soren, 1988), as described in the next paragraph. The overlying Magothy aquifer is not apparent in Richmond Co. (Staten Island).

In NJ (section D–D′ in Fig. 2), sediments of the Cretaceous Potomac Group, Raritan, and Magothy Formations generally have been combined and described as an aquifer system (Gill and Farlekas, 1976; Luzier, 1980). Three mappable aquifer units of varying extent within this "Potomac–Raritan–Magothy (PRM) aquifer system" have been defined as the lower, middle, and upper aquifers, each separated by a confining unit (Zapecza, 1989; Pucci et al., 1994). The middle PRM aquifer, also known as the Farrington Sand Member, appears to be equivalent to the Lloyd aquifer of Staten Island and western Long Island (Zapecza, 1989; Soren, 1988). The middle aquifer consists of fine to coarse sand and locally contains clay beds (Pucci et al., 1994). The upper PRM aquifer of NJ lies unconformably on the Raritan Formation and most nearly corresponds to the Magothy aquifer of western Long Island. It typically consists of marine and nearshore deposits of dark-gray or black clay that contains alternating bands of white micaceous fine-grained sand (Barksdale et al., 1958).

2.2. Groundwater quality

The groundwater systems of Long Island and Staten Island are recharged by precipitation. Recharge near the groundwater divide percolates downward and recharges the deep (Magothy and Lloyd) aquifers, then flows laterally seaward (Misut and Voss, 2007). The

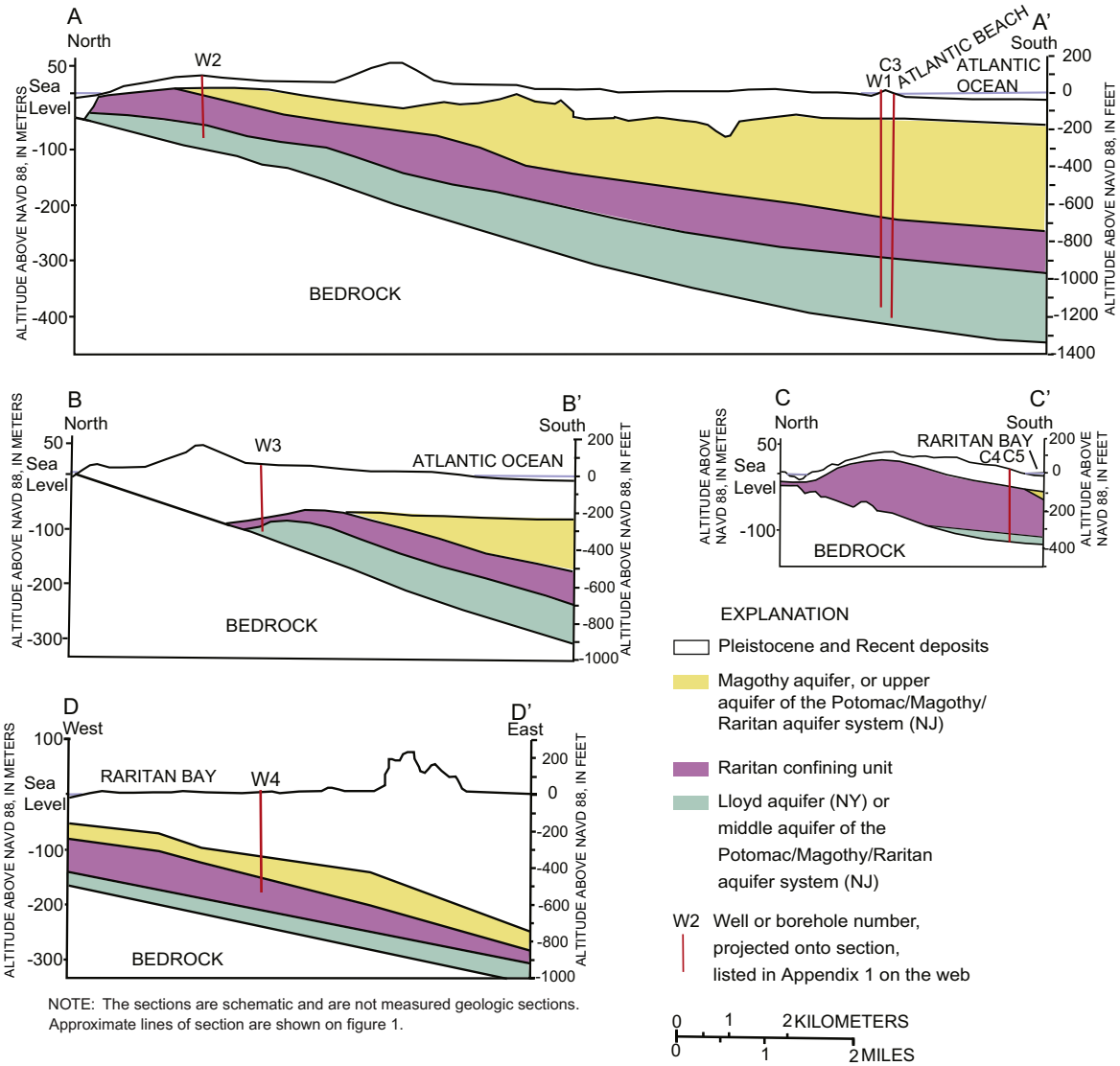

Fig. 2. Hydrogeologic sections A–A′ in Queens County, NY, B–B′ in Kings County, NY (modified from Buxton and Shernoff, 1999), C–C′ in Richmond County (Staten Island), NY (modified from Soren, 1988), and D–D′ in Monmouth County, NJ (modified from Zapecza, 1989).

major ions in Long Island groundwater under predevelopment conditions were Na^+ and Cl^-, and the dissolved-solid concentration was generally less than 50 mg/L (Buxton and Shernoff, 1999). Travel times calculated by a cross-sectional, finite-element model indicate that water in the Lloyd aquifer in central Long Island is several hundred years old (Buxton and Modica, 1992). In Nassau and Suffolk Counties of Long Island, where aquifer deposits typically are deeper than in the NYC area (Fig. 1), DO concentrations in the Lloyd and Magothy aquifers are high near the groundwater divide (recharge area) and decrease along the deep flow paths through redox reactions. Iron concentrations in groundwater samples from these aquifers are highest along the south shore where they typically exceed 0.5 μg/L (Walter, 1997; Brown et al., 2000a). Groundwater has been a source of public supply for western Long Island since the 1850s, but the rapid urbanization of Kings and Queens County since 1900, and the attendant increases in pumping for water supply, have resulted in severe water-level declines and saltwater encroachment.

Concentrations of dissolved inorganic constituents in the Lloyd, Magothy and Jameco aquifers of western Long Island tend to decrease eastward due to decreasing urbanization and supply-well pumping (Buxton and Shernoff, 1999). The encroachment of seawater in response to excessive supply-well pumping has increased concentrations of Cl^-, as well as Ca^{2+} and Mg^{2+}, in the upper glacial aquifer and in parts of the Magothy and Jameco aquifer in much of this area during the past century. Pumping for public supply was terminated in Kings County in 1947 and in western Queens County in 1974. Since pumping ended, water levels have recovered to above sea level and the saltwater has been partly dispersed and diluted. Pumping in eastern Queens County has continued, however, and evidence of a wedge of saltwater moving landward has been reported in southeastern Queens (Buxton and Shernoff, 1999). Chloride concentrations exceeded the SMCL of 250 mg/L in groundwater from many parts of western Long Island (Cartwright et al., 1998). The median specific conductances for groundwater samples from the Lloyd aquifer in Kings, Queens, and Nassau Counties were 301, 175, and 83 μS/cm at 25 °C, respectively, based on water-quality data from the USGS National Water Information System (NWIS) accessed in 2007. Data on dissolved Fe concentrations and other redox indicators in the Lloyd aquifer in Kings and Queens Counties are sparse because there are not many existing Lloyd wells in this area.

Staten Island has four wells that are known to have tapped the Raritan Formation for water supply (Perlmutter and Arnow, 1953), but these were pumped only to supplement city water during periods of drought at rates less than 18.9 million L/d (5 Mgal/d) and were not used after 1970 (Soren, 1988). Water-quality data for wells screened in the Raritan Formation on Staten Island are sparse, although the low potentiometric-head values estimated for 1985 indicate that water from the Lloyd or Farrington equivalent unit of the Rartian Formation could have excessive Cl^- concentrations (Soren, 1988).

In the PRM aquifer system of NJ, groundwater sampled from wells near the regional recharge area in Middlesex County generally is a Na–Ca–SO_4^{2-} water that contains low concentrations of dissolved solids (Ervin et al., 1994). As the water flows through the aquifer, $CaCO_3$ dissolves from calcareous deposits and the water becomes a Ca-HCO_3^- type (Ervin et al., 1994). Supply-well and industrial-well withdrawals along the NJ coastal plain have caused cones of depression and saltwater encroachment that have resulted in the mitigative installation of ASR systems (LaCombe, 1996).

2.3. Suitability of Long Island and Staten Island for ASR systems

ASR would be hydrologically suitable in the Lloyd and Magothy aquifers in Queens, Kings, or Richmond (Staten Island) Counties because they are thick and have large storage capabilities. Aquifers in the NYC area that are deemed hydrologically suitable for ASR were evaluated in this study for possible geochemical processes that could affect ASR implementation and inhibit or enhance recovery efficiency. The Lloyd aquifer, which is thoroughly confined, and the Magothy aquifer, which is mostly confined by a combination of Cretaceous and glacial confining materials, show the most promise for potential development in NYC (Misut and Voss, 2007). However, the Lloyd aquifer beneath Long Island cannot be used for ASR because a law passed in NY in 2008 prohibits the storage or pumping of water into the Lloyd, although the Lloyd aquifer in Staten

Base from New York State Department of Transportation, 1981, and New Jersey Department of Environmental Protection 1:24,0000
Projection Universal Transverse Mercator Projection, NAD 27, Zone 18

Fig. 3. Locations of boreholes, wells, and previously studied sites in the study area of New York city and surrounding areas (Site information is given in web Appendices 1 and 2, and Table 1.)

Table 1
Chemical equations used to describe reactions in Cretaceous aquifers in the vicinity of New York city.

Eq.	Organic C oxidation and reduction of O_2, Mn^{4+}, Fe^{3+}, SO_4^{2-}, and CO_2
1	$CH_2O_{(s)} + O_{2(aq)} \rightarrow CO_2 + H_2O$
2	$CH_2O + 2MnO_2 + H_2O \rightarrow 2Mn^{2+} + HCO_3^- + 3OH^-$
3	$CH_2O_{(s)} + 4FeOOH_{(s)} + 7H^+ \rightarrow 4Fe^{2+} + HCO_3^- + 6H_2O$
4	$2CH_2O + SO_4^{2-} + 2H^+ \rightarrow 2HCO_3^- + H_2S$
5	$2CH_2O \rightarrow CH_4 + CO_2$
	Pyrite oxidation
6	$FeS_{2(s)} + H_2O + 7/2O_{2(aq)} \rightarrow Fe^{2+} + 2SO_4^{2-} + 2H^+$
7	$FeS_{2(s)} + 14\ Fe^{3+} + 8H_2O \rightarrow 15Fe^{2+} + 2SO_4^{2-} + 16H^+$
	Precipitation of $Fe(OH)_3$
8	$Fe^{2+}_{(aq)} + 1/4O_{2(aq)} + H^+ \rightarrow Fe^{3+} + 1/2H_2O$
9	$Fe^{3+}_{(aq)} + 2H_2O \rightarrow FeOOH + 3H^+$
	Siderite dissolution
10	$FeCO_{3(s)} + 2\ H^+ \rightarrow Fe^{2+} + H_2O + CO_{2(g)}$
	Cation exchange pyrite oxidation
11	$Ca^{2+}_{(aq)} + 2NaX_{(ad)} \leftrightarrow 2Na^+_{(aq)} + CaX_{2(ad)}$
12	$Mg^{2+}{}_{(aq)} + 2NaX_{(ad)} \leftrightarrow 2Na^+{}_{(aq)} + MgX_{2(ad)}$
13	$K^+_{(aq)} + NaX_{(ad)} \leftrightarrow Na^+_{(aq)} + KX(ad)$,
	where X(ad) = the ion-exchange site
14	$X- = CEC/(100/sw)(n/(1-n))$,
	where CEC = cation exchange capacity, milliequivalents/100 g dry sediment, sw = specific dry weight of soil, and n = porosity
15	$xFe^{2+} + FeOOH \rightarrow FeOOH_{1-y}Fe_x^{(2X-Y)^+} + yH^+$,
	where x and y are the stoichiometric coefficients for Fe^{2+} sorption and H^+ release (Appelo et al., 1999)

Island remains an option. ASR systems have been installed at several sites on the northeastern NJ coastal plain and may provide some indication of the feasibility for ASR in the NYC area.

3. Methods

Boreholes were drilled and monitoring wells installed in southwestern Nassau County to define the lithology of the Cretaceous deposits through borehole geophysical logging and to collect sediment cores and water samples in anticipation of a possible ASR operation (borehole and well locations are shown in Fig. 3). On Staten Island, two boreholes were drilled, but both collapsed and monitoring wells were never completed. Therefore, water-quality samples were collected from Lloyd wells in western Long Island and compared with previously collected water-quality samples from wells in nearby areas of Long Island and northern NJ (Fig. 3) to provide a basis for interpretation of Staten Island groundwater chemistry.

3.1. Sediment collection and analysis

Solid-phase chemical data from cores collected for this study were compared with core data obtained previously from boreholes at Atlantic Beach in southwestern Nassau County (N10620; D.A. Walter and S.A. Terracciano, USGS, Pers. Comm., 1991), and at Tanner Park in western Suffolk County (Brown et al., 2000a) (Fig. 3). The boreholes and wells completed on Staten Island were drilled by the USGS, and those in Nassau County by the Nassau County Department of Public Works. Sediment cores from Cretaceous deposits were obtained at each of the borehole sites (C1–C3; Fig. 3) during drilling for visual inspection and analysis of mineralogy and grain coatings (for Fe, Mn, As, U, other trace elements), sulfides, and C forms. Five cores from site C4 and five from site C5 (Fig. 3) were selected for analysis; the lithology and mineralogy of these deposits are described in Appendix 1 on the web. Subsamples were removed from the core barrel, then processed (sealed in

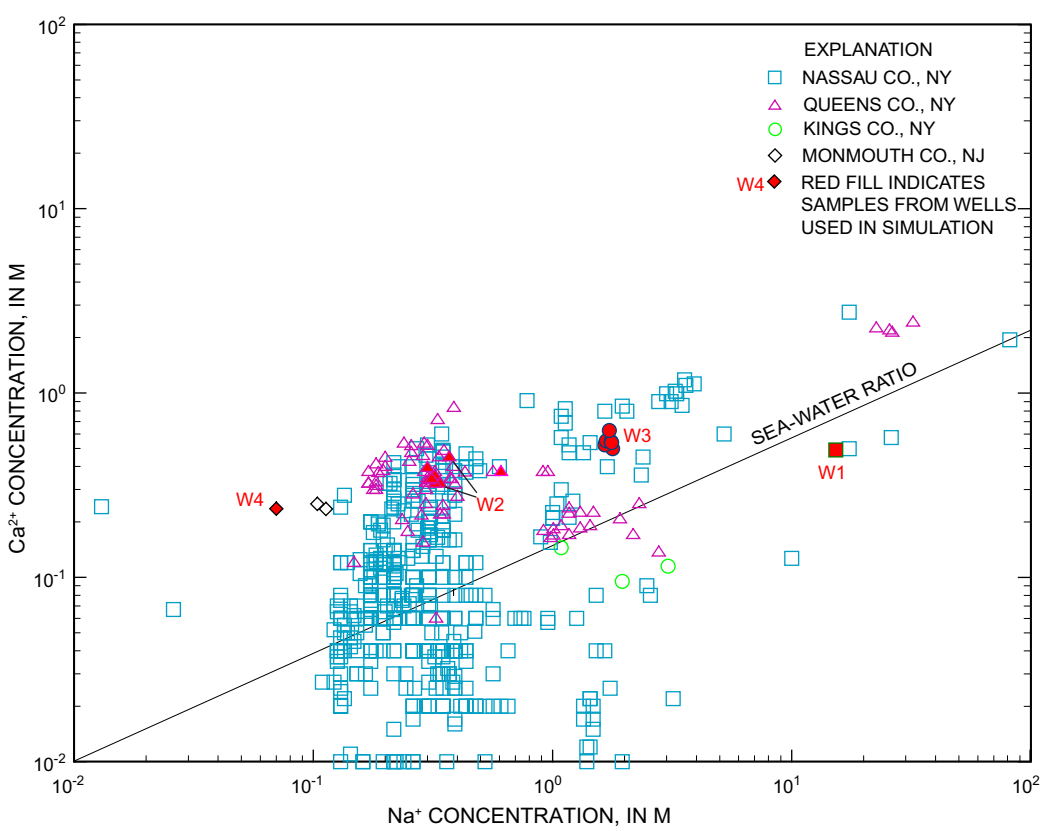

Fig. 4. Ca^{2+} concentrations as a function of Na^+ concentrations in water samples from the Lloyd aquifer on Long Island, NY, and the equivalent Potomac–Raritan–Magothy middle aquifer in northeastern NJ. (General locations are shown in Fig. 3.)

mason jars or ziplock bags) in a glove bag that was continually purged with ultra-pure N_2 gas. Samples were kept on ice or refrigerated prior to analysis.

Core samples were collected for analysis using X-ray diffractometry (XRD), and for element analysis of coating extractions, and C analysis. The mineralogy of bulk samples and clay separates was determined by powder XRD. Sediment pH was measured by first mixing 5 g of soil with 5 mL of distilled water for 10 min., prior to measuring. Total C content was measured by combustion with an automatic C analyzer, and inorganic C content was determined by coulometric titration of acid-evolved CO_2; organic C was computed as the difference between the two values (Arbogast, 1996). The abundance of elements in grain coatings or other mineral phases were identified through treatment by various acids and reagents, including (1) 10% HNO_3, (2) 6 N HCl, (3) 0.5 N HCl–hydroxylamine (HA), and (4) acid volatile and chromium-reducible sulfides extraction, as described in Brown et al. (2009). The coating extraction (HCl and HNO_3) methods were primarily intended to solubilize ferric oxyhydroxides and (or) associated trace elements, but they also can extract other oxides and clay, carbonate, and sulfide phases to varying degrees. The 6 N HCl-extractable Fe (total) fraction indicates the amounts of crystalline and poorly crystalline Fe coating and generally is 2–10 times greater than the 0.5 N HCl–HA-extractable Fe, which indicates the amount of poorly crystalline Fe(III) in the sample, presumably, the most microbially reactive Fe fraction. Leachate derived from the 10% HNO_3 extractions was analyzed by ICP–OES. Analysis of the 6 N HCl extractants required dilution to 1.6 N HCl prior to analysis by ICP-MS. The 0.5 N HCl–HA and 6 N HCl extractions were done in accordance with the method of Lovley and Phillips (1987) and analyzed by colorimetry and ICP-MS, respectively.

3.2. Groundwater sample collection and analysis

Groundwater samples were collected at wells 1 and 2 in Queens County, well 3 in Kings County, and well 4 (collected previously) in northeastern NJ (Fig. 3) and analyzed for a broad suite of analytes, including water temperature, specific conductance, pH, DO, major and trace elements, As species, nutrients, ^3H, and stable isotopes of O, H, S and C. Several of these parameters are included in Appendix 2 on the web, but were not used as model input parameters. Wells were purged, and temperature, specific conductance, pH, turbidity, and DO concentrations were monitored until stable. Concentrations of total dissolved sulfide (H_2S and HS^-) and DO (below 1 mg/L) were measured onsite using colorimetric procedures. Alkalinity was measured by incremental titration within a few hours of sample collection. Concentrations of major ions, trace elements, and nutrients were measured in samples filtered with a 0.45-μm inline filter. Groundwater SO_4^{2-} was collected on an anion-exchange resin column for S-isotope analysis, or if SO_4^{2-} concentrations were sufficiently high, the water was collected in a bottle. Water samples for $\delta^{13}C$ analysis of dissolved inorganic C (DIC) were collected in 1-L glass bottles, which were filled from the bottom up and sealed with a Teflon/silicon septum cap, 3–5 L were allowed to overflow to eliminate oxygen. Dissolved-gas samples were collected in 160-mL septum bottles and sealed within a large beaker overflowing with groundwater from the well.

The water samples were analyzed by the USGS National Water-quality Laboratory (NWQL) in Denver, CO for major ions, trace elements, nutrients, dissolved organic C (DOC), Rn, pesticides and volatile organic compounds. Major ions and trace elements were analyzed by inductively coupled plasma/mass spectrometry, atomic absorption spectrometry, or ion chromatography. Nutrient concentrations were measured by colorimetry, and DOC was analyzed by ultraviolet-promoted persulfate oxidation and infrared spectrometry.

3.3. Geochemical modeling

Two models were used to simulate geochemical reactions associated with ASR, including PHREEQC (Parkhurst and Appelo, 1999), a one-dimensional model, and PHAST (Parkhurst et al., 2004), a 3-dimensional reactive-transport model. Different scenarios and geochemical conditions were first investigated with 1-D forward geochemical modeling using PHREEQC to establish the primary geochemical reactions, which were then included in 3-D reactive-transport modeling. In PHAST, the combined flow, transport, and geochemical processes are simulated by three sequential calculations for each time step: first, flow velocities are calculated; then, the chemical components are transported; and finally geochemical reactions are calculated Parkhurst et al., 2004).

Table 3
Simulated duration, rate, and total volume of water injection and extraction at hypothetical ASR sites in the New York city study area of NY and northeastern NJ.

Rest period (years 0–1)	Injection (years 1–6)	Storage period (years 6–7)	Extraction (years 7–15)
Rate	6.89×10^8 L/a	–	13.82×10^8 L/a
	(1.82×10^8 gal/a)	–	(3.65×10^8 gal/a)
Total volume	3.45×10^9 L	–	1.11×10^{10} L
	(9.1×10^8 gal)	–	(2.92×10^9 gal)

Table 2
Concentrations of selected constituents in groundwater samples on which chemistry of injectate and groundwater at hypothetical ASR sites in study area were based. [mM, millimoles per liter; μM, micromoles per liter; DO, dissolved oxygen.]

Injectate or well ID	Description/location	pH	DO (mM)	HCO_3^- (mM)	Na^+ (mM)	Ca^{2+} (mM)	Fe, dissolved (μM)	Mn, dissolved (μM)
Injectate A	NYC water	7.2	0.22	0.16	0.31	0.14	0.54	0.15
Injectate B	NYC water reacted with Na_2CO_3, equilibrated. with atmospheric CO_2, O_2	7.5	0.37	4.2	0.43	0.14	<0.12	0.15
W1 (N13565)	Nassau County	6.6	<0.006	0.43	15	0.49	85	4.2
W2 (Q2420.1)	Queens County	6.7	0.028	1.5	0.3	0.39	50	2.3
W3 (K3410.1)	Kings County	7.6	0.013	2.9[a]	1.7	0.55	20	2.2
W4 (250639)	Monmouth County, NJ	6.2	0.006	1.1	0.1	0.25	180	2.8

[a] Estimated by difference in charge balance.

Table 4
Median, mean, and range of Fe and Fe sulfide concentrations estimated from selected acid extractions from Cretaceous aquifer cores in Richmond and Nassau Counties, NY, and baseline concentration values used in the PHAST model of a hypothetical ASR site. [Concentrations are in moles per liter, *M*.]

Selective extraction	Median	Mean	Range	Model input
0.5 N HCl–HA extractable Fe	0.007	0.11	0.0025–1.2	0.1
6 N HCl-extractable Fe	0.036	0.14	0.01–1.1	
Fe sulfides	0.020	0.023	0.0016–0.08	0.001

Results of PHAST simulations were visualized by using a modified version of the Model Viewer software (Hsieh and Winston, 2002).

Hydraulic parameters used in PHAST simulations were based on those obtained in a previous study that used the 3-dimensional, density-dependent groundwater flow and solute transport model SUTRA (Misut and Voss, 2007) to develop regional representations of groundwater flow and saltwater–freshwater interface movement in Kings and Queens Counties. The hydraulic parameters calibrated in the SUTRA model were applied to the PHAST models, and were as follows: horizontal hydraulic conductivity, 30 [m/day]; vertical hydraulic conductivity, 3 [m/day]; porosity, 0.25; and specific storage, 3×10^{-6} [1/m]. A flat hydraulic gradient was simulated within the model domain with constant-head boundary conditions of 0 m on opposite sides of the model. During transient simulations, a fully penetrating well (50-m length) placed in the center of the model domain for injection of NYC water for 5a, followed by a 1-a pause preceding 8a of extraction through pumping. This hypothetical injection/recovery scenario corresponds to an operation schedule envisioned by NYC to mitigate a supply deficiency due to long-term temporary shutdown of a major

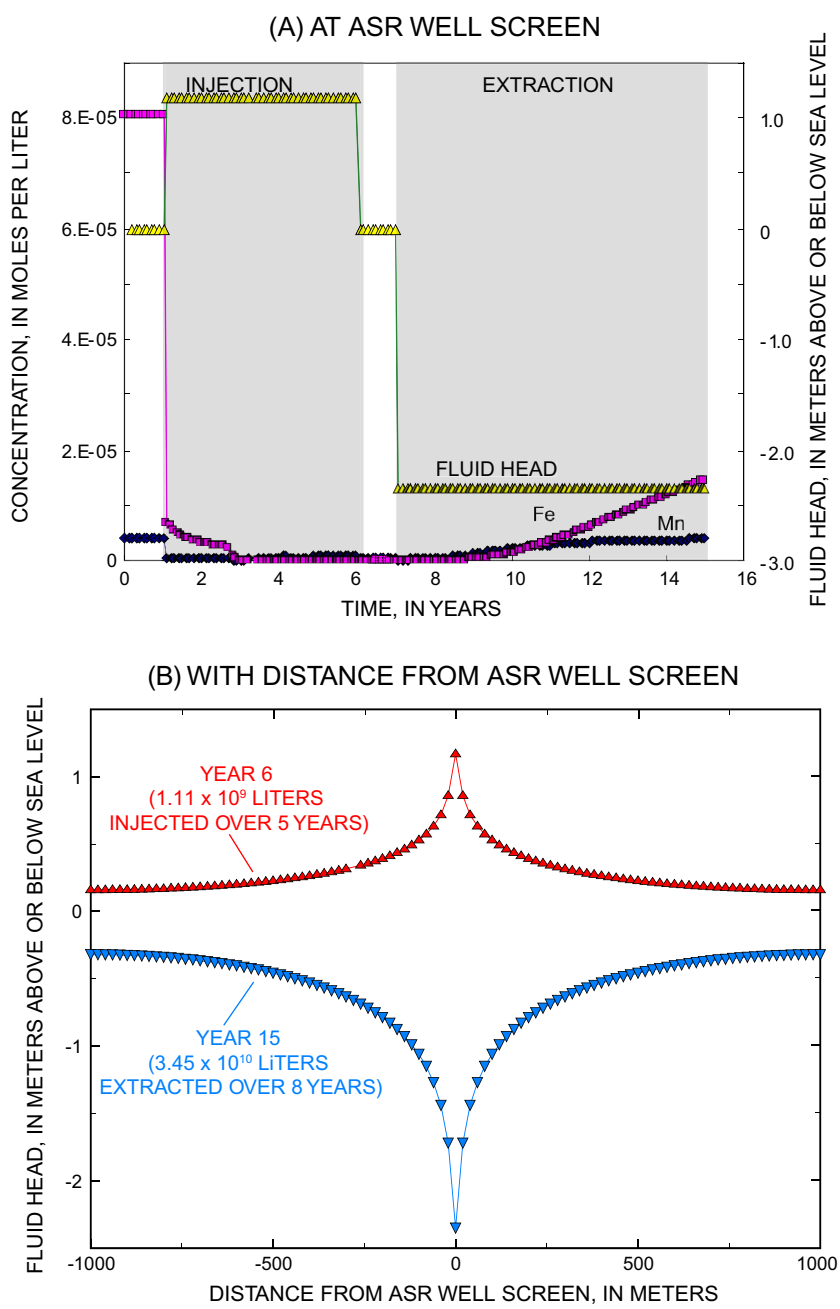

Fig. 5. Simulated A. Fluid head and concentrations of dissolved Fe and Mn at hypothetical ASR well during the ASR cycle for the baseline scenario, and B. Fluid head as a function of distance from the well screen at year 6 (after 5a of injection) and at year 15 (after 8a of extraction).

water-supply tunnel for maintenance. The model scenario used in this study also provides sufficient (1) injectate travel distance and (2) periods of injection and extraction to assess the geochemical processes discussed in this paper. Injection resulted in the formation of a mound in the potentiometric surface, that, during the extraction phase, declined and became a cone of depression that gradually propagated outward. The maximum distance that an injectate particle traveled from the ASR well during the simulation was about 25% of the length of a model domain side (2000 m).

4. Results and discussion

Both the solid-phase chemistry and groundwater chemistry are critical to understanding chemical processes that affect the ASR design. Data on solid-phase chemistry of core samples from the Cretaceous deposits of Staten Island and Long Island were compared with data from cores previously collected elsewhere on Long Island to ascertain differences or similarities in the mineralogy, organic matter content, and lithology. Similarly, the chemistry of groundwater samples from several wells was compared with data from samples previously collected elsewhere on Long Island and northeastern NJ to ascertain differences or similarities. The groundwater data from most wells on Long Island and northeastern NJ generally indicated low concentrations of major and minor constituents, although specific conductance ranged from about 30 μS/cm at inland locations to more than 2000 μS/cm in coastal areas that are affected by saltwater intrusion (Appendix 2 on the web).

4.1. Solid-phase chemistry

Most of the cores analyzed for mineralogy and acid-extractable concentrations of Fe, Mn, As, Pb, Cd, Cr, Cu, U, and other constituents were from borehole sites C4 and C5 on Staten Island (22); only three of the cores were from western Long Island (Appendix 1 on the web), but these data were supplemented by previously collected core data from other parts of Long Island and NJ.

The lithology of Cretaceous deposits at the Staten Island borehole sites C4 and C5 (Fig. 3) ranged from sand and gravel, to silty clay, to clay interspersed with zones containing considerable amounts of lignite and Fe-sulfide minerals (pyrite or marcasite). The XRD of whole-sample powder mounts from Cretaceous deposits indicated the predominance of quartz with some feldspars, including plagioclase and K feldspar, mica (generally muscovite), total clay, pyrite, goethite, and amphibole. The feldspar composition generally is between andesine and oligoclase, or about 30% anorthite. Iron-sulfide minerals typically were associated with lignite and silt and clay deposits. Sediment-extracted sulfides, which ranged from 100 to 3000 μg/L, coincided with pyrite in samples observed visually or measured by XRD, and were inversely associated with Fe^{3+} (Appendix 1 and 2 on the web). The low sediment pH (3.2–6.2) indicates, however, that pyrite is dissolving in some locations where Fe oxides are present because pyrite can be oxidized by dissolved Fe^{3+} ions under low pH conditions (see Eq. (7), Table 1); Murowchick and Barnes, 1986). Although oxidation of Fe^{2+} (see Eq. (8), Table 1) is the rate-limiting step for pyrite oxidation by Fe^{3+} (Singer and Stumm, 1970), Fe-oxidizing bacteria such as *Thiobacillus ferrooxidans* are able to increase the Fe^{2+} oxidation rate as much as five orders of magnitude, similar to the rate of pyrite oxidation by Fe^{3+} (Nordstrom, 1982). Therefore, in the presence of Fe-oxidizing bacteria and O_2, the oxidation of Fe^{2+} to Fe^{3+} may no longer be the rate-limiting step for pyrite oxidation by Fe^{3+}. Other Fe-bearing minerals, including goethite, amphibole, chlorite, and staurolite were detected in some bulk samples, and goethite and chlorite were detected in some clay fractions (Appendix 1 on the web). Glauconite was observed at the two Staten Island sites (C4, C5, Fig. 3) and indicates a transitional-marine depositional environment. Kaolinite and illite generally were the primary clay minerals (<1 μm

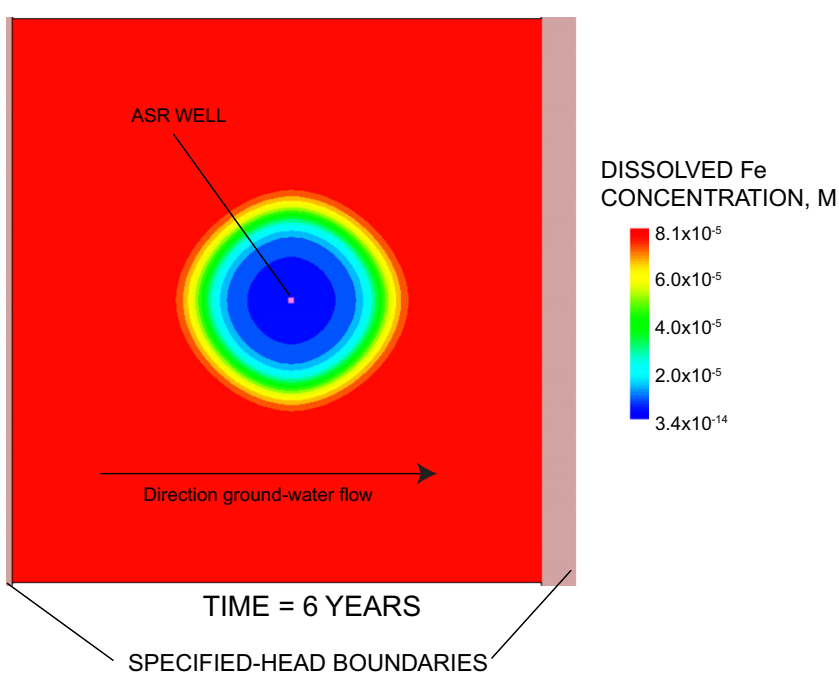

Fig. 6. Model representation of dissolved Fe concentrations at the ASR well screen at year 6 (after 5a of injection) for the baseline scenario.

fraction) in addition to smectite, intergrade smectite, chlorite and goethite.

Carbonate minerals are scarce in Staten Island and Long Island Cretaceous deposits (Appendix 1 on the web), although siderite ($FeCO_3$) was found near the bottom of the unnamed clay member of the Raritan Formation on Long Island (Brown et al., 1999) and in northeastern New Jersey (Pyne, 1995). Given the abundance of SO_4^{2-} in Atlantic Coastal Plain deposits (Pucci et al., 1992; Brown and Schoonen, 2004) and the paucity of carbonate minerals, the formation of siderite is less likely than the formation of Fe-sulfide minerals (Postma, 1982).

Extractable concentrations of Fe and Mn, particularly their oxic forms associated with grain coatings, can be used to assess the redox environment of the part of the aquifer from which the sample was taken. Concentrations of 0.5 N HCl–HA extractable Fe (total) coatings ranged from 98 to 44,000 μg/g, and the relatively high concentrations of Fe^{2+} and sulfides indicate that sediments generally are anoxic, as expected (Appendix 1 on the web). The similar range in 6 N HCl-extractable Fe concentration (360–40,000 μg/g of sample) indicates that the poorly crystalline, presumably microbially reactive, 0.5 N HCl–HA extractable Fe^{3+} in these sediments is a small fraction of the total extractable Fe (Appendix 1 on the web). Concentrations of 6 N HCl extractable Mn coatings (<0.2–2300 μg/g of sediment) were much lower than those of 6 N HCl-extractable Fe (total) coatings (Appendix 1 on the web), and generally were consistent with relative concentrations of dissolved Fe and Mn in groundwater. Concentrations of trace elements extracted from some core samples indicated that concentrations of Fe, Mn, and acid volatile sulfides (AVS) plus chromium-reducible sulfides (CRS) could be high in reduced sediments, but extractable concentrations of As, Pb, Cd, Cr, Cu, and U were low. The 10% HNO_3-extractable As and Cd concentrations correlated positively with sedimentary sulfide concentrations, but Pb showed a negative correlation. U concentrations in 6 N HCl extractions were highest (1 μg/g and 6.6 μg/g) near bedrock at both the C4 and C5 boreholes on Staten Island (Appendix 1 on the web).

4.2. Groundwater chemistry

Geochemical conditions in the Lloyd and Magothy aquifers of the study area can vary locally, and are summarized here briefly. Groundwaters of four types typical of the study area are represented by samples from the following sites (locations are shown in Fig. 3):

- W1 (well N13565) Lloyd aquifer, Nassau County: salty, moderate pH, high Fe.
- W2 (well Q2420) Lloyd aquifer, Queens County: moderate pH, high Fe.
- W3 (well K3410) Lloyd aquifer, Brooklyn, Kings County: moderate pH, high Fe, HCO_3^-.
- W4 (well 250639) Magothy–Raritan–Potomac aquifer system (MRPA) undifferentiated, Monmouth County, New Jersey: Ca–HCO_3^-–SO_4^{2-} water, low pH, high Fe.

The major-ion chemistry of water from the Magothy and Lloyd aquifers on Long Island reflects a generally Na–Cl water in recharge areas which changes to a Ca–Na–Mg–HCO_3^- water along groundwater flow paths (Appendix 2 on the web). Groundwater samples from the Lloyd aquifer in Nassau County had median specific conductance of 83 μS/cm, but ranged as high as 2250 μS/cm in areas affected by saltwater intrusion and are represented by a groundwater sample from well W1 (Appendix 2 on the web). Coastal areas with saltwater intrusion have a Na–Cl hydrogeochemical facies that results from the mixing of fresh groundwater with seawater or brackish water (Fig. 4).

The pH of groundwater samples in Nassau County was low-to-moderate (4.2–8.2), and the water was undersaturated with respect to calcite (Appendix 2 on the web) as were most other water samples from the Lloyd aquifer. Groundwater quality further west in Queens and Kings Counties is as listed for wells W2 and W3 above, respectively. Groundwater chemistry in Staten Island is generally only known in the shallow system because the deep aquifer is not used for public drinking-water supply (Soren, 1988). Groundwater in the Cretaceous upper, middle, and lower aquifers of the PRM aquifer system in northeastern NJ generally is a Ca–Mg–HCO_3^- water in areas of recharge and evolves to a

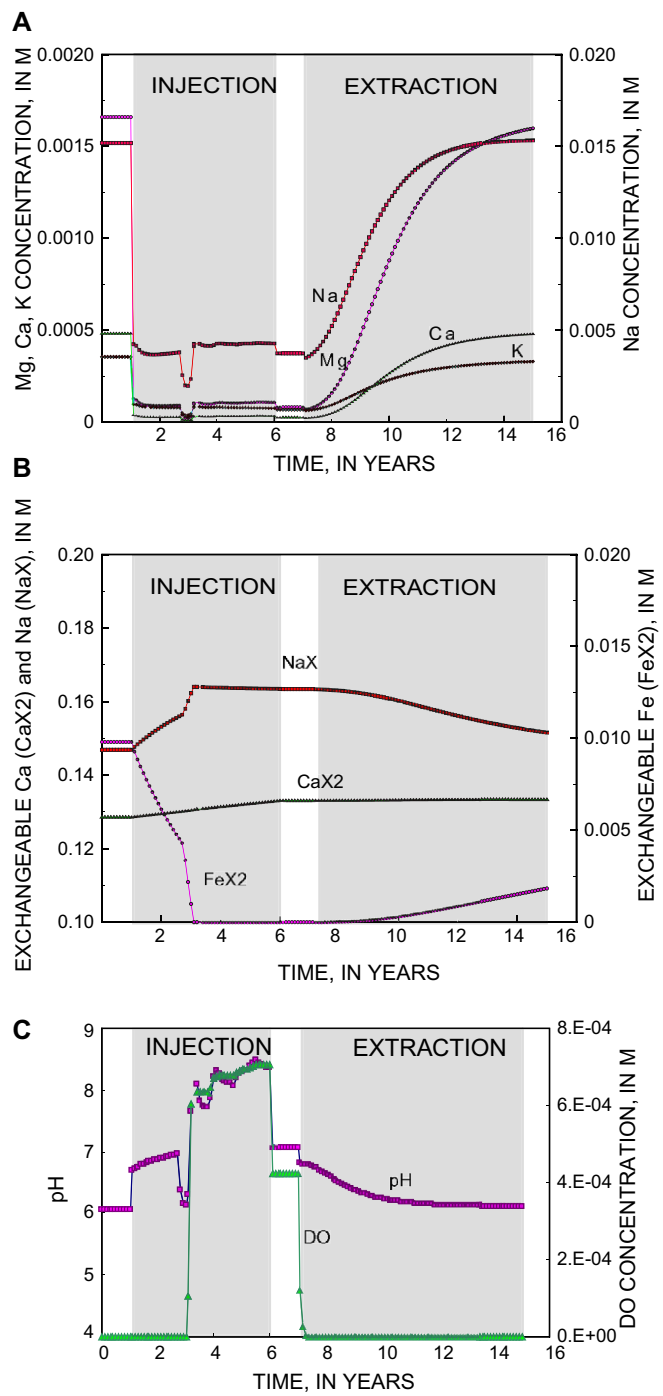

Fig. 7. Simulated chemical concentrations at the ASR well screen for the 15-a baseline scenario: A. Dissolved Mg^{2+}, Ca^{2+}, Na^+, and K^+ in water. B. Exchangeable cations NaX, CaX_2, and FeX_2 on aquifer sediments. C. pH and dissolved O_2 in water.

Na–HCO_3^- water along groundwater flow paths (Knobel et al., 1998). The change is primarily due to ion exchange and aquifer weathering. Well W4 in Monmouth County, NJ, is a Ca–HCO_3^-–SO_4^{2-} water with a high concentration of dissolved Fe.

Much of the information on geochemical processes associated with the Lloyd and Magothy aquifers of central Long Island (Brown et al., 2000a) can be applied to those Cretaceous aquifers in western Long Island and Staten Island. Increases in concentrations of dissolved Fe, Mn, and HCO_3^- along flow paths in the Cretaceous (Lloyd and Magothy) aquifers of Long Island have been associated with the reduction of dissolved O_2 (referred hereafter as "DO"), Mn^{4+}, Fe^{3+}, and SO_4^{2-} coupled to lignite oxidation (Eqs. (1)–(5) in Table 1). Calcite dissolution is unlikely to contribute to the DIC increase because the Magothy and Lloyd aquifers of Long Island contain little or no carbonate minerals. The reduction of CO_2 to CH_4 (Eq. (5) in Table 1) occurs under sufficiently reducing conditions, and CH_4 was present in some wells. The oxidation of organic matter by SO_4^{2-} reduction is represented by Eq. (4) in Table 1. Alternatively, localized anaerobic zones associated with lignite and Fe-sulfide minerals (FeS_2) are common in oxic parts of Cretaceous aquifers in the Long Island area (Brown et al., 1999) and FeS_2 may become oxidized by DO and (or) Fe^{3+} (Eqs. (6)–(8)) (McKibben and Barnes, 1986; Moses et al., 1987). The low solubility of Fe^{3+} may require Fe^{3+}-reducing organisms to come into direct contact with Fe^{3+}-bearing solids (Lovley, 1987), unless either the Fe^{3+} is complexed with other compounds (e.g., Lovley et al., 1996), or the pH is low enough (<~3) that Fe^{3+} is soluble. Evidence of oxidized Fe-sulfide minerals in aquifer sediments of eastern Long Island includes low pH (e.g., 4.4), isotopically light $\delta^{34}S$ of SO_4^{2-} in water from some public-supply wells, and etched pyrite in aquifer sediments (Brown et al., 2000a). In other areas where redox gradients exist, such as near public-supply wells, oxidation of Fe^{2+} to Fe^{3+}, and subsequent precipitation of FeOOH (goethite) (Eqs. (8) and (9)) and similar reactions with Mn result in encrustation and biofouling of well screens (Walter, 1997). These reactions produce protons, which slow the rate of oxidation. Although siderite has been found sporadically and its dissolution (Eq. (10)) could contribute locally to high concentrations of dissolved Fe in groundwater, siderite is not supersaturated in groundwater samples studied here (Appendix 2 on the web) as reported in other anaerobic aquatic environments (Jensen et al., 2002).

Sodium–Ca exchange can occur as freshwater flows through Cretaceous sediments that were deposited under nonmarine- to transitional marine conditions, and through other Cretaceous deposits into which saltwater intrusion has been induced through overpumping. In this process, aqueous Ca^{2+} is exchanged for Na^+ on exchange sites. Groundwater from well W1, in southwestern Nassau County (Fig. 3), has higher concentrations of Na^+ and lower

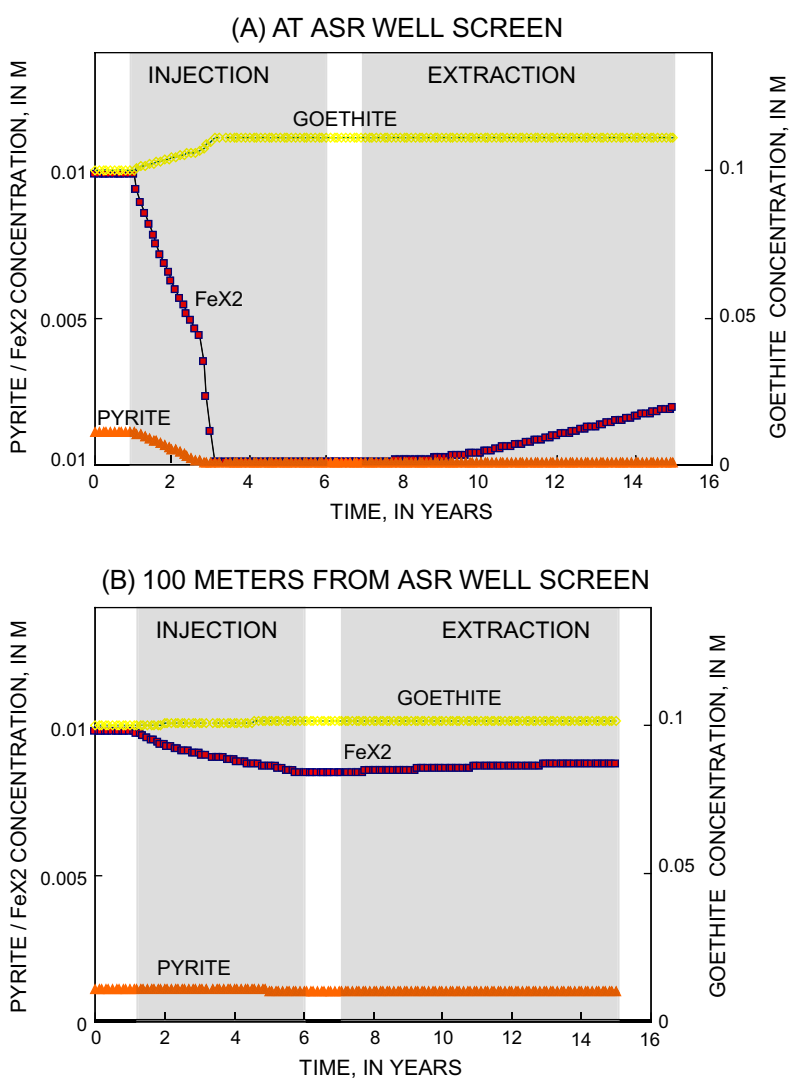

Fig. 8. Simulated concentrations of exchangeable Fe (FeX_2), goethite, and pyrite for the 15-a baseline scenario: (A) at the ASR well screen. (B) At 100 m from the ASR well screen.

concentrations of Ca^{2+} than groundwater from upgradient wells (Fig. 4). The Lloyd aquifer on Long Island has lower Ca:Mg ratios, and lower (Na + K):Mg or (Na + K):Ca ratios than the upper glacial aquifer and Magothy aquifer; these low ratios reflect the high exchange capacity of the overlying Raritan confining unit (Lani and Schoonen, 1996; Brown and Schoonen, 2004). The Ca^{2+}–HCO_3^- water from well W4 in northeastern NJ could indicate some dissolution of calcite, although the HCO_3^- concentrations are not high relative to those in the other samples (Appendix 2 on the web). Higher dissolved concentrations of Ca^{2+} than those of Na^+ in groundwater near the saltwater interface can indicate seawater intrusion, whereas higher concentrations of Na^+ than of Ca^{2+} in such areas typically indicates intrusion of freshwater into sediments that were previously saturated with seawater (Appelo and Postma, 1993) and has caused the attendant cation-exchange reactions (Eqs. (11)–(13)). Furthermore, high HCO_3^- concentrations in groundwater in near-shore areas where seawater has advanced, and the high concentrations of Ca^{2+} that have exchanged for Na^+ in seawater in these areas, can cause near saturation with respect to calcite. The higher alkalinity in these areas, therefore, could affect ASR efficacy by decreasing the solubility of goethite and resulting in Fe^{3+} encrustation around the screen.

4.3. Simulations of ASR scenarios

ASR for hypothetical wells screened in Cretaceous aquifers was simulated by using PHAST in a simplified conceptual model. The model domain is in a sand layer 2000 m in length and width and 50 m thick. The model grid has a point-distributed mesh, such that the edges of the model are defined by nodes. Cell faces are placed halfway between the nodes in each direction. The model grid was discretized with 101 nodes at 20-m spacings in the *X* and *Y* directions and with two nodes at 25-m spacing in the *Z* direction. A hydraulic conductivity value of 30 m/day was assigned to the aquifer. The model domain geometry was generalized into a flat layer of constant thickness, even though the Cretaceous aquifers in the study area are gently sloping and of variable thickness (Fig. 2) and likely to contain (1) layers of coarse-grained deposits with relatively low ion-exchange capacity through which there will be preferential flow of injected water, and (2) layers of fines with lower permeability, higher exchange capacity and potentially higher concentrations of Fe-sulfide minerals and greater acidity. The boundaries were assigned a constant head and constant chemical concentration boundary conditions.

The constant-head/constant concentration boundary conditions are simplified representations of potential ASR sites. Changes in head or water quality at these boundaries could result from pumping or other nearby hydrologic stresses, or from regional factors such as movement of the freshwater/saltwater interfaces. Nevertheless, the model can help evaluate geochemical processes that may affect the quality of water recovered during ASR, and the efficiency of the process, in this type of hydrogeologic setting.

The hypothetical injectate is derived from city (NYC) water that originates from reservoirs in upstate New York. New York city

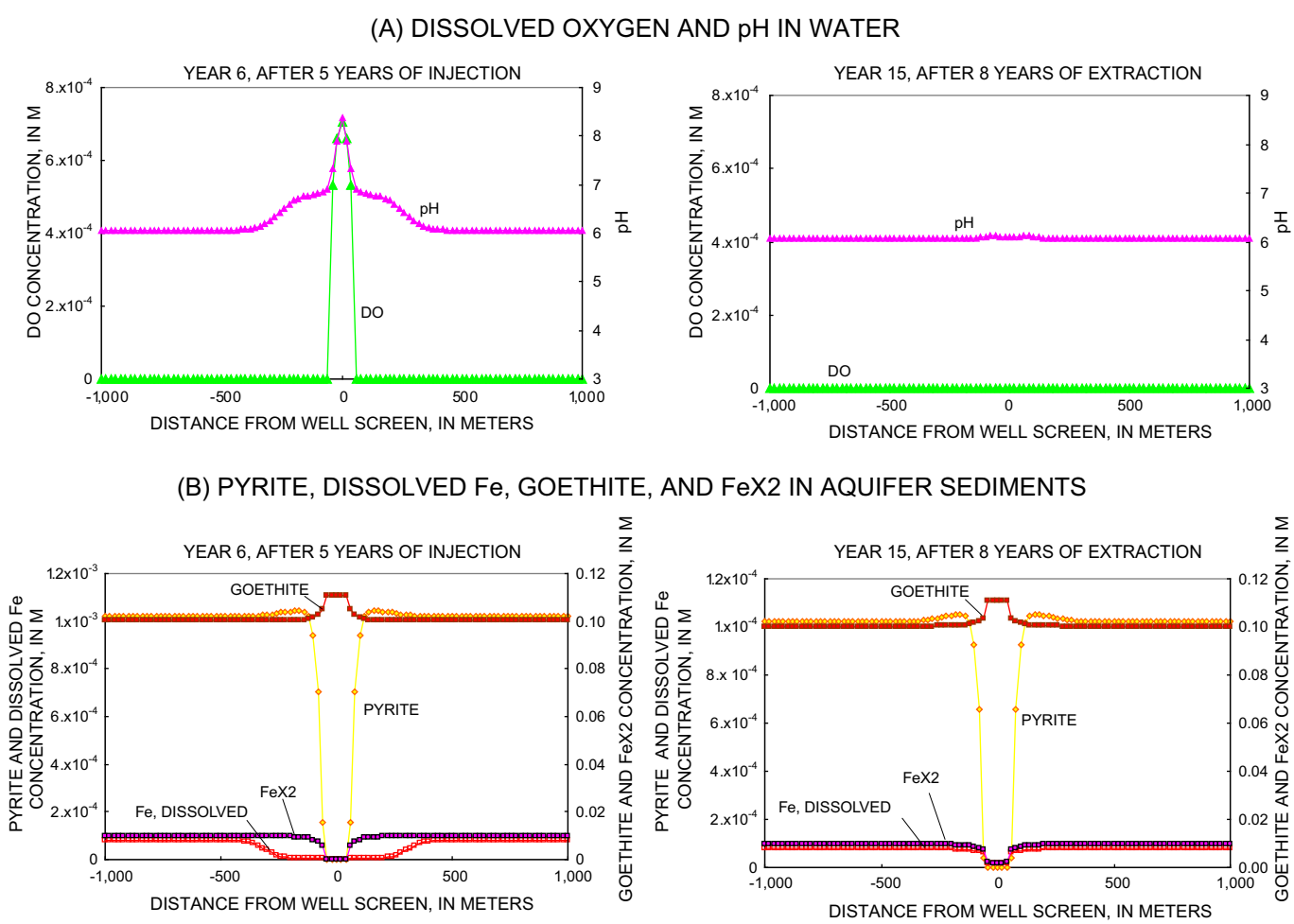

Fig. 9. Simulated concentrations of selected constituents in water and aquifer sediments with distance from the ASR well screen after 5a (year 5) of injection and after 8a of extraction (year 15) for the baseline scenario: A. DO and pH in water. B. Pyrite, goethite, dissolved Fe and exchangeable Fe (FeX_2) in aquifer sedments.

water has low ionic strength and generally is of high quality, and was represented in the model by water-quality data collected in 2001 (NYCDEP, 2002). A buffer is commonly added to acidic injectate in ASR applications to prevent corrosion of distribution lines; therefore two types of injectate were simulated, both of which were equilibrated with atmospheric CO_2 and O_2 in the PHREEQC module of PHAST. Injectate A was defined as unbuffered NYC water, and Injectate B was defined as NYC water that was reacted with 2 mM/L Na_2CO_3 (Table 2).

The following describes the simulated injection, storage and recovery of water at a hypothetical ASR well. The aquifer is initially equilibrated for a period of 1 a prior to injection, then the injectate is pumped into the well at a rate of 6.89×10^8 L/a for 5a (Table 3). Injectate B (Table 2) was used for the baseline scenario. At year 6, injection is stopped for 1a, and then the well is pumped at a rate of 13.82×10^8 L/a for 8a until the end of the 15-a period. The simulated time required to remove one well volume was 0.5 day. Typically, a small volume of injected water is left in the aquifer during each cycle to ensure that any precipitates such as ferric hydroxide do not plug the formation near the well screen (Pyne, 1995); however, these simulations remove a volume greater than the volume injected (Table 3).

4.3.1. Baseline scenario

For simplicity, a single well in Nassau County (site W1, well N13565) was used for the baseline ASR scenario in which NYC water was injected for a 5-a period, and then extracted for 8a after a 1-a pause. The aquifer mineralogy used in the model represented

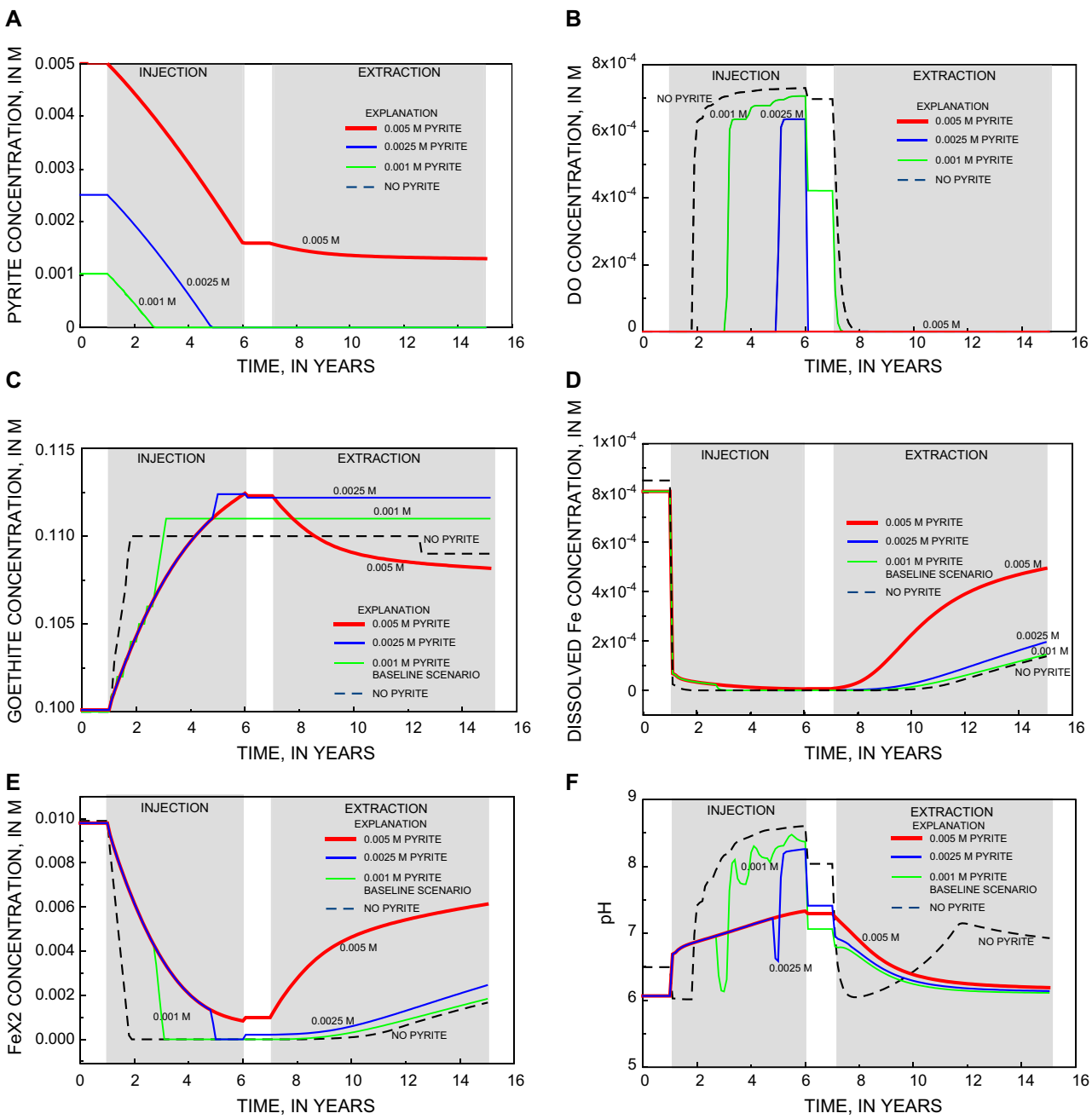

Fig. 10. Simulated concentrations of selected constituents at the ASR well screen during scenarios with 4 different pyrite concentrations: A. Pyrite. B. Dissolved oxygen (DO). C. Goethite. D. Dissolved Fe. E. Exchangeable Fe^{2+} (FeX_2). F. pH.

the indicated core samples from Cretaceous deposits in Richmond and Nassau Counties (Table 4). Concentrations of Fe and Fe sulfides in extracts from the core samples (Appendix 1 on the web) were used to obtain baseline concentrations of reactive Fe-bearing minerals used in the ASR site model. Extractable concentrations (μg/g; Appendix 2 on the web) were converted to dissolved concentrations (μg/L) by factoring in an estimated bulk density (*BD*) of aquifer sediments (1.8 g/cc). The baseline concentration of goethite (0.1 M) used in the model was obtained from the mean concentration of total 0.5 N HCl–HA-extractable in core sediments (Table 4), as adjusted for the estimated *BD*. The baseline concentration of Fe sulfide (pyrite) used in the model (0.001 M) was below the range estimated from extractable Fe sulfides (AVS + CRS) in core sediments (Table 4), but probably more realistic because much of the observed pyrite was associated with poorly permeable sediments and not as likely to be mobilized as the pyrite in the sand fraction. Furthermore, model-input concentrations for pyrite were varied among simulations, as discussed in the next section "Baseline scenarios with varied pyrite concentrations". Concentrations of goethite were defined as 0.1 M in the baseline model, based on converting the extractable Fe concentrations to dissolved concentrations using the estimated bulk density. Siderite was included in a separate simulation of the NJ site (well W4), as discussed in the section "Baseline scenarios with varied groundwater chemistry" section below. The amount of ion exchanger, X^- (Eq. (14) in Table 1) was calculated from estimates of porosity (*n*) and specific weight (*sw*) of 0.3 and 2.65 g/cm^3, respectively, and a median cation exchange capacity (CEC) of 16.8 meq/100 g, as reported for Cretaceous deposits on Long Island (Brown and Schoonen, 2004), to obtain a value of 1.0 equivalents (Eq. (14) in Table 1). The default database for PHAST contains thermodynamic data for hydrous ferric oxide (Hfo) on a particle surface; the values are derived from Dzombak and Morel (1990), who defined a strong binding site (Hfo_s) and a weak binding site (Hfo_w) and used 0.2 M per mol Fe for weak sites and 0.005 M for strong sites, a surface area of 5.33×10^4 m^2/M Fe, and a gram-formula weight of 89 g Hfo per mol Fe. The geochemical processes in the aquifer around the hypothetical ASR well screen were found to vary during injection and extraction. The reactions and changes in concentrations of solid, sorbed, and dissolved constituents associated with ASR injection and recovery in the baseline scenario are discussed below.

4.3.1.1. Injection phase. The simulated injection of buffered NYC water (injectate B, defined in Table 2) into the hypothetical ASR well increased the hydraulic head around the ASR well screen (Fig. 5A and B), displaced the ambient groundwater, and formed a spheroid with concentrations of Fe and Mn (Fig. 5A and 6) and major cations (Fig. 8A) in the vicinity of the well that were lower

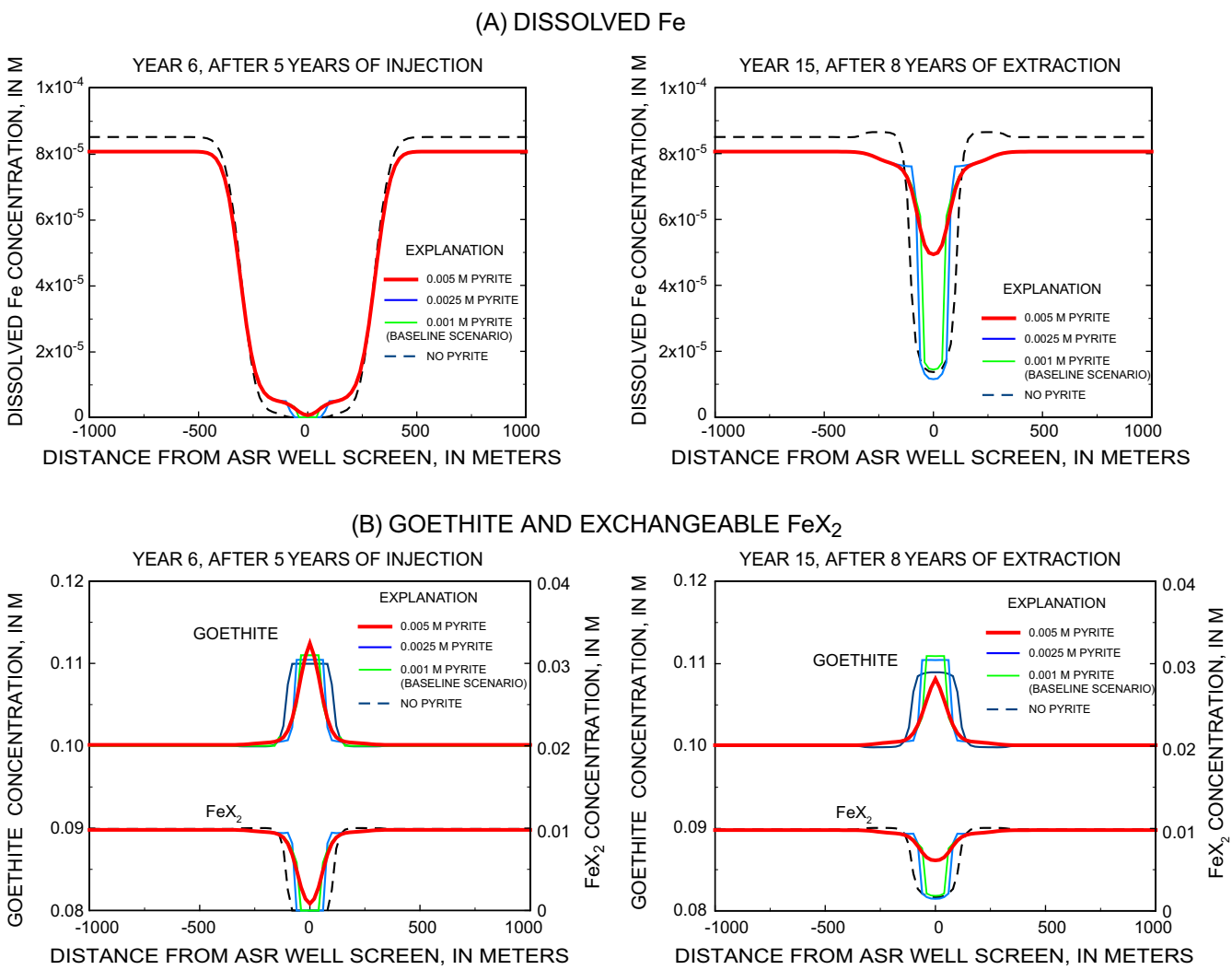

Fig. 11. Simulated concentrations of dissolved Fe, goethite, and exchangeable Fe (FeX_2) as a function of distance from the ASR well screen after 5a of injection (year 5) and after 8a of extraction (year 15), during scenarios with four different pyrite concentrations: A. Dissolved Fe. B. Goethite and exchangeable Fe (FeX_2).

than in the ambient water. The dilution of dissolved-cation concentrations at the well screen was accompanied by the exchange of dissolved cations for cations on aquifer solids (Fig. 7A and B). All cations were diluted by the injectate except H^+, which increased as other cations were sorbed. Dissolved Na^+ and Ca^{2+} also exchanged for FeX_2 on aquifer solids during the injection phase (Fig. 7A and B) and the pH and DO concentrations at the well screen generally increased during injection (Fig. 7C). Pyrite dissolved (Fig. 8) through oxidation by O_2 (Eq. (6) in Table 1) under the oxic conditions of the injectate water and the Fe^{2+} from pyrite oxidation, together with exchangeable Fe^{2+} (FeX_2), oxidized to form goethite (Fig. 8A; Eqs. (8) and (9) in Table 1). As the pyrite dissolved, Fe^{2+} from FeX_2 was oxidizing by about the same amount, although the dissolution of pyrite generated less acidity per mol of O_2 than the oxidation of Fe^{2+} in FeX_2. After all of the pyrite (0.001 M) had dissolved (year 2.7), only the FeX_2 oxidation continued, and the pH dropped (Fig. 7C) because oxidation of Fe^{2+} and formation of goethite (Fig. 8A) produced more H^+ per mol of O_2 consumed than did pyrite oxidation. The DO began to increase at year 3.1, but only after the cessation of O_2-consuming reactions of pyrite oxidation, Fe^{2+} oxidation, and goethite precipitation. Goethite precipitated until dissolved Fe was depleted after about 3.2a. Beyond a distance of 100 m from the ASR well screen, less pyrite (0.0001 M) dissolved and less Fe desorbed, than at the well screen, but these reactions continued throughout the duration of the ASR cycle (Fig. 8B). At the end of the injection cycle, DO concentrations and pH near the ASR well screen were high (Fig. 9A) and reflected the injectate chemistry. Concentrations of dissolved Fe after injection remained low, but had migrated farther from the well screen (about 400 m) (Fig. 9B). Concentrations of pyrite and FeX_2 within 40 m of the ASR well were depleted or negligible and at distances of 40–100 m from the ASR well were partly depleted, whereas goethite in this same vicinity had precipitated (Fig. 9B).

4.3.1.2. Extraction phase. Dissolved and exchangeable Fe^{2+} (FeX_2) near the well increased as the extraction pumping drew ambient water with high dissolved Fe concentrations back toward the well (Figs. 5A and 7C). Dissolved Fe^{2+} in water from outside the spheroid of injectate was sorbed onto goethite (Eq. (15) in Table 1) when the flow was reversed; this was first observed by Van Beek and Vaessen (1979) and described in detail by Appelo et al. (1999). After the 8a of simulated extraction, the lowered hydraulic head had created a cone of depression (Fig. 5B). The lower concentrations of dissolved Fe (1.4×10^{-5} M) in the extracted water (11.1 billion L) than in the relatively small amount of water injected (3.45 billion L) into this aquifer with high Fe concentrations (4.6×10^{-5} M), exemplifies the efficiency of the reactions associated with the resulting in situ Fe removal. The concentrations of dissolved and exchangeable Fe within 40 m of the ASR well screen remained relatively low, despite the extraction of three times more water than was injected (Table 3) and despite the fact that DO within this zone was depleted (Fig. 9B). The concentrations of dissolved Fe in this zone were less than 1.7×10^{-6} M (or 1 mg/L) throughout the extraction period (Fig. 9B) and remained below 5.4×10^{-6} M (or 0.3 mg/L), the SMCL for drinking water (USEPA, 2008), until 11.7a (after 4.7a of

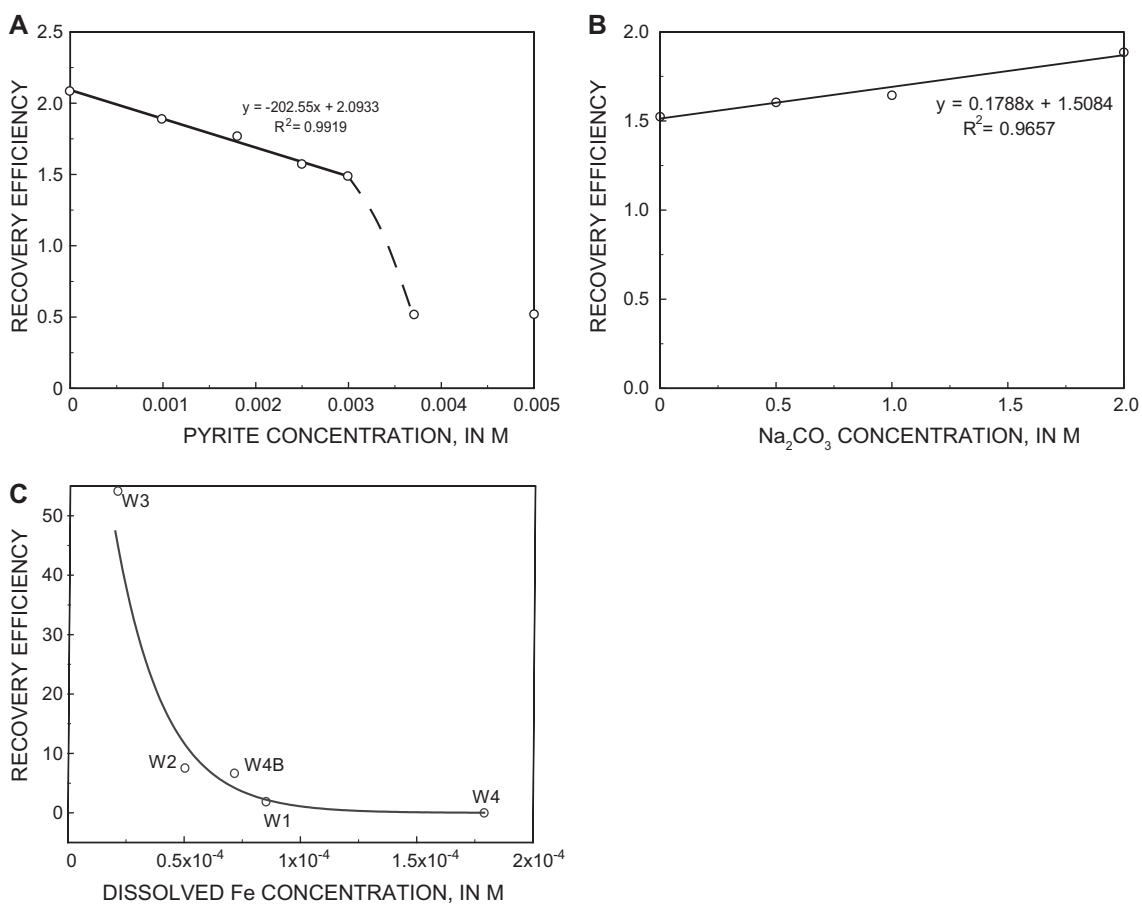

Fig. 12. Recovery efficiency (volume extracted with dissolved Fe concentrations below 5.4×10^{-6} M divided by the volume injected) for simulations with varying concentrations of: A. Pyrite. B. Buffer (Na_2CO_3). C. Dissolved Fe for groundwater samples for sites W1 , W2, W3 , W4 (without siderite), and W4B (with a low dissolved Fe concentration of 7.2×10^{-5} M, or 4 mg/L. (Well locations are shown in Fig. 3.)

extraction). At this Fe concentration, about 88% more water can be extracted than was injected. As discussed earlier, the sorption of dissolved Fe^{2+} onto precipitated goethite results in a net loss of dissolved Fe in the aquifer. During pumping, concentrations of NaX decreased as the high concentrations of dissolved Fe in ambient water were drawn toward the well and exchanged for NaX (Fig. 7B). The concentration of dissolved Fe increased at about year 9, or 2a after the start of extraction, and continued to increase to the end of the simulation (Fig. 5B). Less pyrite (0.0001 M) had dissolved at a distance of 100 m from the well screen than near the well, but pyrite dissolution continued throughout the duration of the ASR cycle (Fig. 8B). Pyrite oxidation, goethite precipitation, and FeX_2 exchange were affected to a distance of about 400 m from the well screen (Fig. 9B). Note that pyrite reached saturation and a small amount precipitated beyond the oxic region caused by the injectate (Fig. 9B).

A sensitivity analysis was done to discern which variables had the greatest effect on dissolved Fe concentrations in extracted water, including saltwater intrusion at well W1 in southwestern Nassau County. Four constant parameters in the baseline scenario:- the concentration of pyrite, the concentration of the injectate buffer, the groundwater chemistry, and the addition of siderite, were varied through a range of values. Additional simulations in which only the groundwater chemistry was varied were used to model the other three hypothetical ASR locations, including well W2 (Q2420) in Queens County, well W3 (K3410) in Kings County, and well W4 (250,639) in Monmouth County, NJ, for a comparison of their water quality. All four wells were chosen to represent a range of chemistry, including groundwater affected by salt water intrusion at the baseline scenario (W1).

4.3.2. Baseline scenario with varied pyrite concentrations

The concentration of pyrite in aquifer sediments was varied to indicate the effect of pyrite dissolution on goethite precipitation and dissolved Fe concentrations. Pyrite concentrations of zero, 0.001 M (the lower range of extraction estimates used in the baseline scenario, Table 4), 0.0025 M and 0.005 M were applied to simulations (Fig. 10A), and the response of the concentrations of selected constituents and pH were plotted through time (Fig. 10B through E) and over distance from the well at year 6 (after 5a of injection) and at year 15 (after 8a of extraction) (Fig. 11). The successively larger amounts of pyrite applied to the model caused a corresponding decrease in the duration in the DO peak, and the simulation with the highest pyrite concentration (0.005 M) resulted in the depletion of all the DO injected (Fig. 10B). The maximum amount of pyrite dissolved was 0.0037 M. The less DO that is available to oxidize Fe^{2+} and precipitate goethite (Fig. 10C), the less goethite will be available to sorb Fe^{2+} in ambient groundwater being drawn back toward the well during extraction, and the higher will be the concentrations of dissolved Fe in extracted water (Fig. 10D). Concentrations of goethite generally were lowest, and the concentrations of dissolved Fe and FeX_2 generally were highest in simulations with the highest concentrations of pyrite (Figs. 10C–E and 11A and B). More exchangeable Fe^{2+} near the well results in more oxidation and restricts the movement of DO into the aquifer (Fig. 10B). The effect of pyrite dissolution on the amount of goethite and pH is important for recovery efficiency; the lower pH that is associated with successively larger concentrations of pyrite (Fig. 10F) results in higher goethite solubility (Figs. 10C and 11A), lower sorptive capacity of goethite for Fe^{2+} (Fig. 10E), and higher

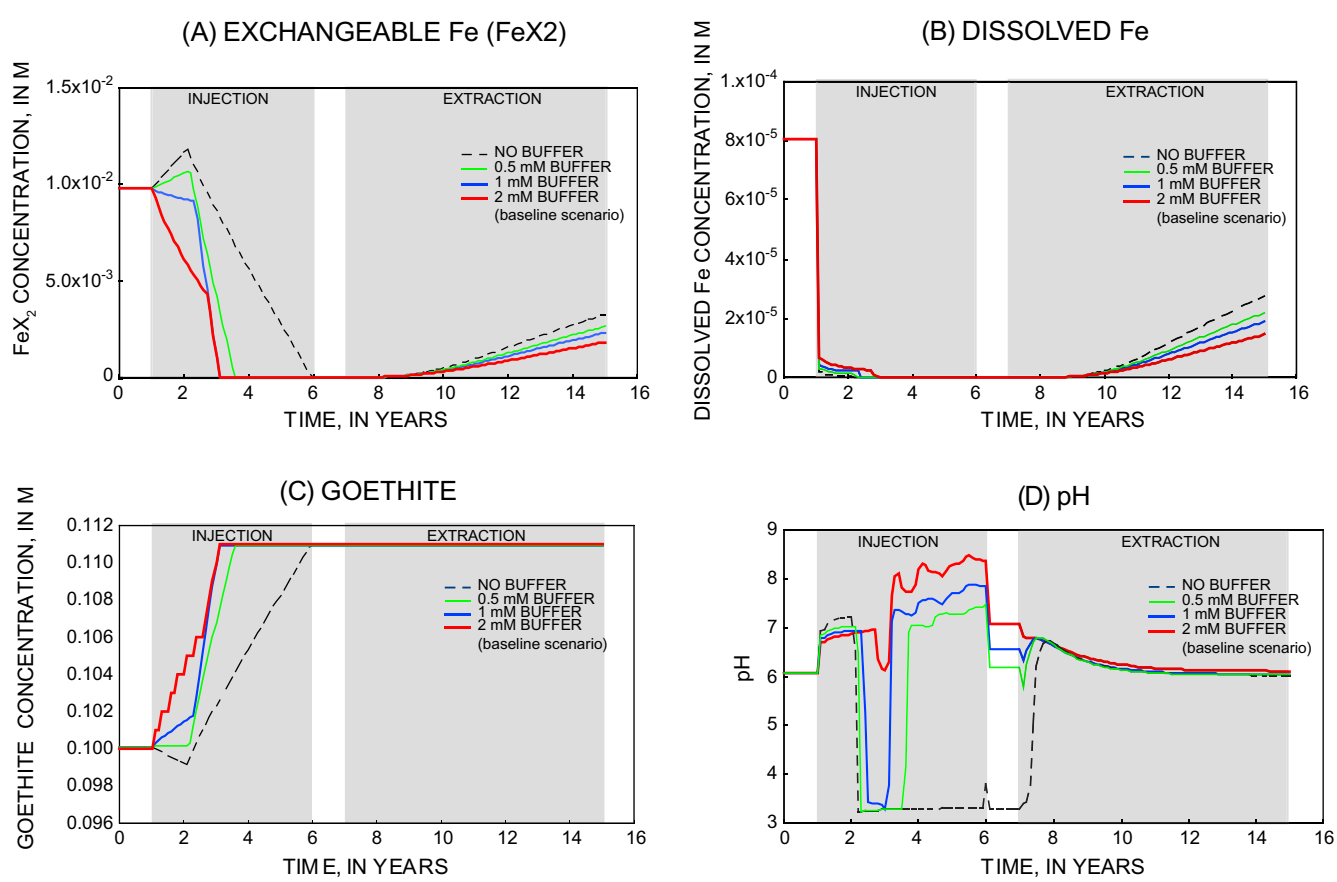

Fig. 13. Simulated concentrations of selected constituents in aquifer sediments at the ASR well screen during extraction scenarios with varied concentrations of injectate buffer (Na_2CO_3). A. Exchangeable Fe (FeX_2). B. Dissolved Fe. C. Goethite. D. pH.

concentrations of dissolved Fe during later stages of the extraction phase (Figs. 10D and 11A). The addition of pyrite, and its oxidative dissolution, to ASR simulations result in decreased volumes of extractable water with dissolved Fe concentrations below the SMCL of 5.4×10^{-6} M (Fig. 12A). The linear decrease in recovery efficiency that resulted from the successively greater pyrite concentrations, and subsequent dissolution, results from the depletion of DO and the increase in acidity. Simulations with more than 0.0037 M of pyrite, the maximum amount dissolved in the baseline scenario, had just over a 50% recovery efficiency.

The PHAST model assumes that all reactions are at equilibrium, but does not take into account microbial activity or the formation

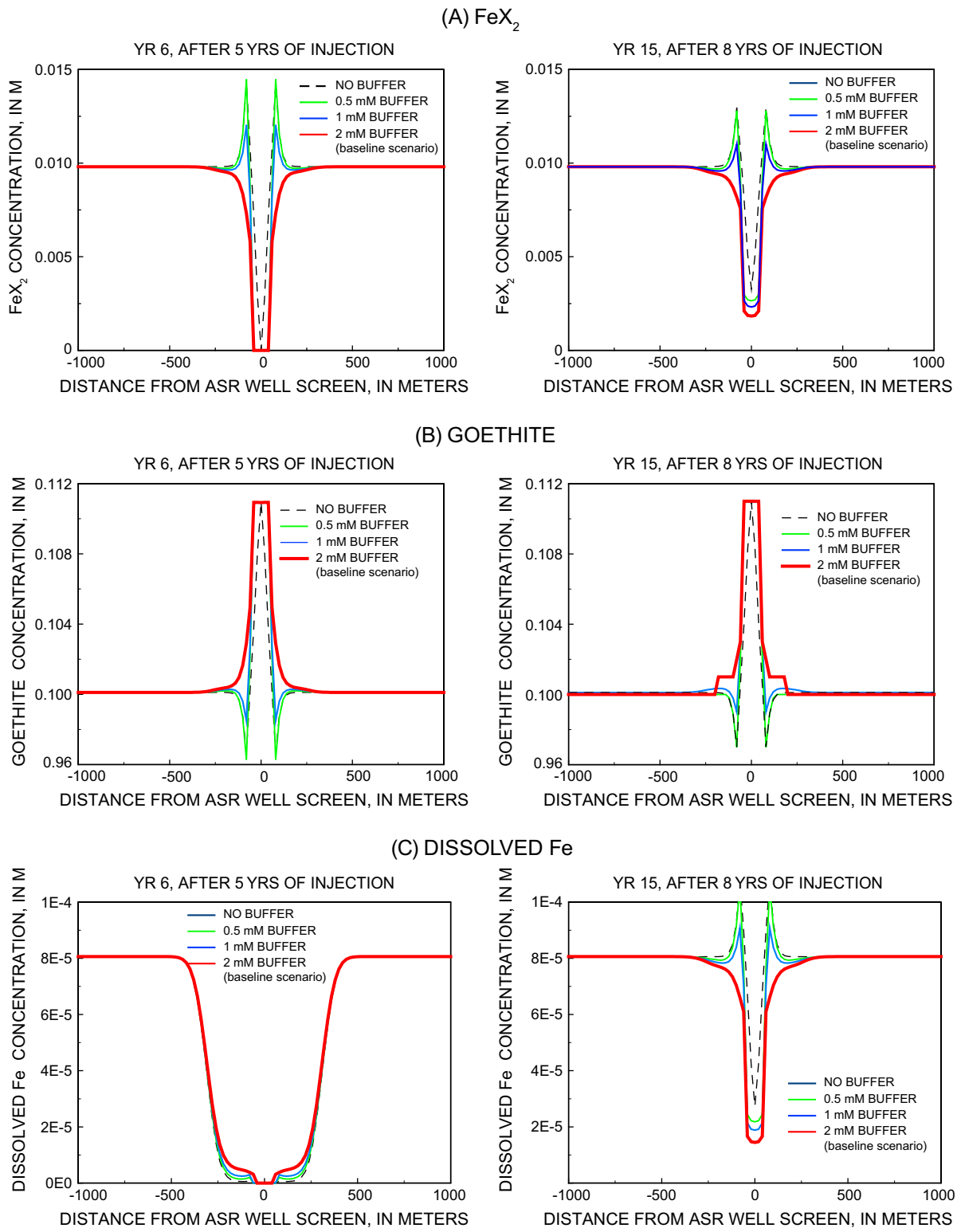

Fig. 14. Simulated concentrations of selected groundwater constituents with distance from the ASR well screen after 5a of injection (year 6) and after 8a of extraction (year 15), in scenarios with varied concentrations of injectate buffer (Na_2CO_3): A. Exchangeable Fe (FeX_2). B. Goethite. C. Dissolved Fe.

of biofilm associated with goethite precipitation on and around the well screen. The extent of Fe^{2+} oxidation per injectate volume was greater at moderate pH, although the reaction (Eq. (9) in Table 1) produced protons, which in turn decreased the extent of reaction when the injectate was unbuffered. The model simulation assumes Fe^{2+} oxidation to be instantaneous in the injectate part of the aquifer, but this is not unreasonable considering that Fe^{2+} oxidation is rapid, and on the order of 3×10^{-6} mol/L/a under oxic, abiotic conditions (Dempsey et al., 2001); this would equate to over 3200 mol/a during the simulated injection period if O_2 was not limiting. The rates for oxidation of organic matter (Eq. (1) through (5)) and pyrite (Eqs. (6) and (7)) are much slower than the Fe^{2+} oxidation, and the O_2-rich water injected into an aquifer will preferentially consume Fe^{2+} (Appelo et al., 1999).

4.3.3. Baseline scenario with varied buffer concentrations

4.3.3.1. Injection phase. The concentration of buffer in injectate B (as defined in Table 2) was varied from the baseline scenario of 2 mM Na_2CO_3, to simulations with no buffer to simulations with concentrations of 0.5 mM and 1 mM. The greater the buffer con-

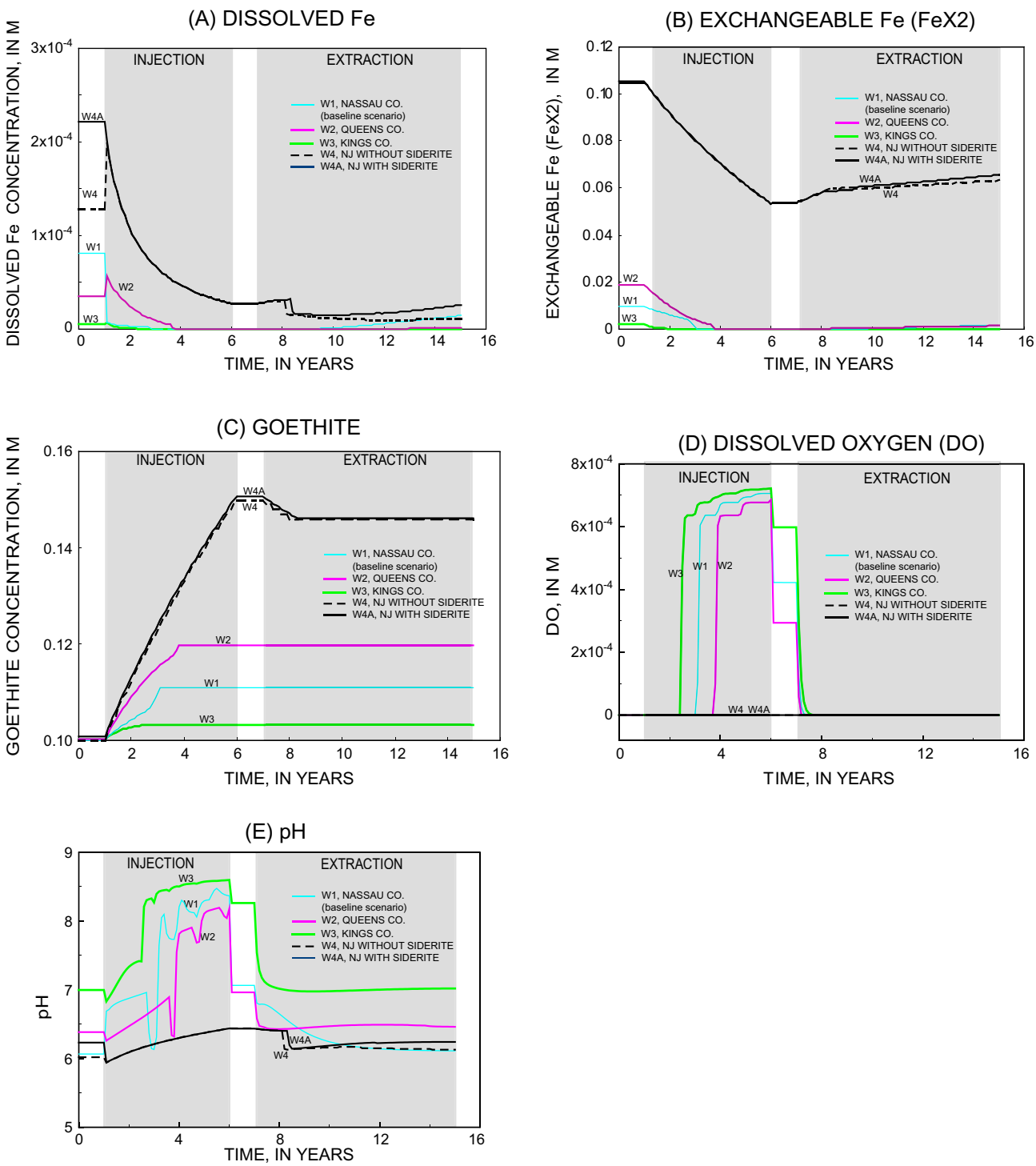

Fig. 15. Simulated concentrations of: A. Dissolved Fe. B. Exchangeable Fe (FeX_2). C. Goethite. D. Dissolved oxygen (DO). E. pH at the hypothetical ASR well screen for scenarios with groundwater from well samples in Nassau (baseline scenario), Kings, Queens Counties, NY, and Monmouth County, NJ. (Well locations are shown in Fig. 3.)

centration in the injectate, the greater the release of exchangeable Fe from sorption sites (Figs. 13A and 14A) for dissolved cations such as Na^+, and the higher the concentrations of dissolved Fe and goethite during injection (Fig. 13B and C) and after injection (Fig. 14B and C) compared to simulations with less or no buffer in the injectate. Concentrations of FeX_2 in scenarios with the buffer were depleted over a greater distance from the well screen after injection than in the scenario without the buffer (Fig. 14A). In the buffered simulations, goethite precipitates over a shorter part of the injection period due to the similarly more rapid depletion of FeX_2 and the relatively low solubilities that exist under the higher pH conditions compared to those in the unbuffered simulation (Fig. 13A, C and D). Goethite also precipitated over a greater distance from the ASR well screen in the buffered simulations because FeX_2 depletion extended farther from the well screen and because the pH was slightly higher, compared to simulations with less or no buffer in the injectate (Fig. 14A–C).

4.3.3.2. Extraction phase. During the extraction phase (9–15a), more ambient Fe^{2+} is sorbed onto goethite as water is drawn toward the well in the buffered simulations, and dissolved Fe concentrations are lower compared to the unbuffered scenario (Figs. 13B and 14C). After 2a of extraction (year 9), dissolved Fe concentrations are higher in the unbuffered scenarios despite similar pH values (Fig. 13A and D) and reflect the high concentrations of cation exchange complexes (NaX) other than FeX_2; these high dissolved Fe concentrations indicate that ASR systems that use poorly buffered injectate could require Fe treatment after extraction. The pH (Fig. 13D) and concentrations of DO generally are slightly higher with successively higher concentrations of Na_2CO_3 buffer in the injectate and with distance from the ASR well screen; this higher pH will favor the sorption of Fe^{2+} onto goethite during extraction. The percentage of sorption sites increased with a change in pH from 7 to 8, for example, because the positive charge on Hfo decreases when the point of zero charge (PZC = 8.3) is approached (Appelo et al., 1999). The greater degree of FeX_2 exchange provided by the buffered injectate allows FeX_2 exchange, which moves well beyond the DO front, to proceed farther from the well screen and results in more goethite precipitated farther into the aquifer (Fig. 14A and B) than would occur without the buffer. Successively increased amounts of buffer added to the injectate, therefore, increase the recovery efficiency of ASR (Fig. 12B), although the magnitude of sensitivity is not as great as with varying the pyrite (Fig. 12A).

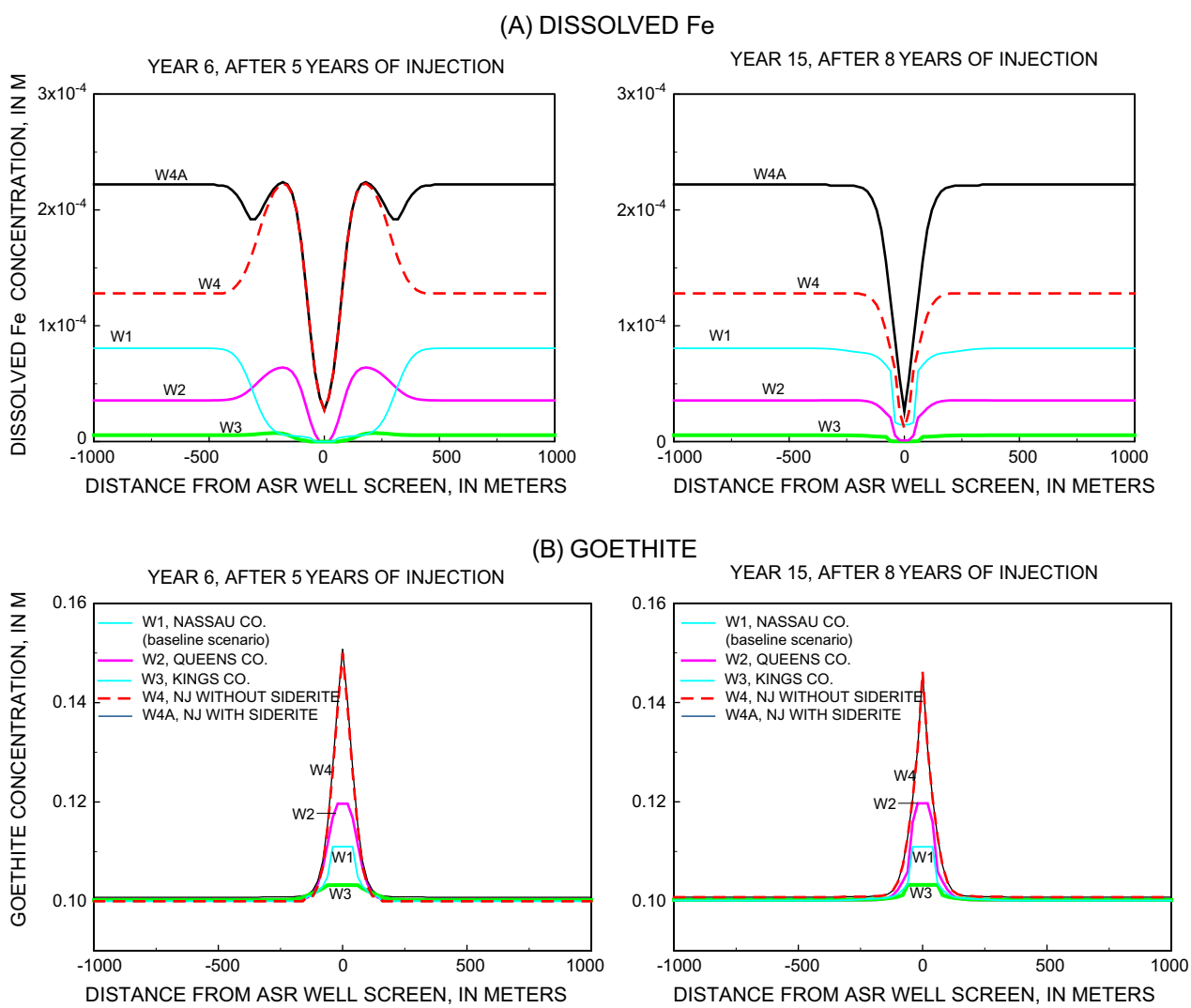

Fig. 16. Simulated concentrations of selected groundwater constituents with distance from the ASR well screen after 5a of injection (year 6) and after 8a of extraction (year 15) for groundwater samples for sites W1 (Nassau Co., or baseline scenario), W2 (Queens Co.), W3 (Kings Co.), W4 (Monmouth Co., NJ, without siderite), and W4A (with siderite): A. Dissolved Fe. B. Goethite. (Well locations are shown in Fig. 3.)

4.3.4. Baseline scenario with varied groundwater composition

Concentrations of dissolved Fe in ambient groundwater differ among the 4 study sites, and decrease through precipitation of goethite and sorption of Fe^{2+} during the ASR cycle (Fig. 15A). Concentrations of dissolved FeX_2 at W1 (baseline site) were low relative to other sites (Fig. 15B) as a result of the high concentrations of sorbed complexes, such as NaX and CaX_2 that are associated with saltwater intrusion at W1. After injection, water near the well screen at the W1 site had lower concentrations of dissolved Fe (Figs. 15A and 16A) than at W2, farther inland, despite having higher concentrations of dissolved Fe in ambient water. Site W3 (in central Kings County), which had the lowest concentrations of dissolved Fe (2.0×10^{-5} M) and FeX_2, also had the smallest amount of goethite formed (Fig. 15C), despite the higher concentrations of DO than at the other sites (Fig. 15D). Site W4 (in northeastern NJ) had the highest dissolved Fe concentration of any site (0.18 M, Fig. 15A); the addition of 0.001 M of siderite as an equilibrium phase at this site (termed W4A) resulted in the highest dissolved Fe concentrations at the beginning and end of the cycle (Figs. 15A and 16A), as expected from the higher solubility of siderite than of other Fe phases in the aquifer. The concentrations of dissolved (Fig. 15A) and exchangeable Fe^{2+} (Fig. 15B) and goethite (Fig. 15C) acted as redox buffers at sites W4 and W4A and the DO concentration (Fig. 15D) did not increase appreciably during the injection phase, nor did the pH (Fig. 15E) because H^+ was released during precipitation of goethite (FeOOH) (Eq. (9) in Table 1). The lowest concentrations of DO at sites other than W4 and W4A were at the baseline (W1) site and at W2 (Fig. 15D), where DO consequently oxidized the least amount of pyrite (not shown in figure). Pyrite dissolution progressed over a longer period at W4 (about 8a) than at the other sites because more Fe^{2+} oxidizes, thereby decreasing the availability of oxidants (e.g., O_2) required for oxidative dissolution reactions (Eq. (6) in Table 1). The pH at site W1 generally is higher than that at site W2 during and after injection (Fig. 15E), probably because the exchange of H^+ for the high concentrations of sorbed complexes at W1 results in a decrease in the solubility of goethite.

After extraction, the W1 site again had higher concentrations of dissolved Fe in the vicinity of the ASR well screen than did W2 (Figs. 15A and 16A), after ambient groundwater was drawn back toward the well. The amount of goethite formed at W2 was greater than at W1 because the amount of exchangeable Fe^{2+} at W1 that could be oxidized to Fe^{3+} and precipitated was comparatively small; also, the pH of water at W1 decreased relative to that at W2, and thereby contributed to the greater solubility of goethite at W1. As a result, less dissolved Fe was sorbed onto goethite at W2 than at W1 (Fig. 16A). Site W3 had a low ambient dissolved Fe concentration that never exceeded the SMCL during the simulation and would have required 140a of cation exchange to exceed the SMCL. The greatest amounts of goethite precipitation in the vicinity of any well screen were at sites W4 and W4A (the well at which siderite was added); this resulted in the lowest pH of all sites after 5a of extraction (Fig. 15E).

The high concentrations of dissolved Fe in ambient groundwater were a major factor in recovery efficiency at all wells (Fig. 12C), and the simulated recovery efficiencies declined exponentially with increases in the concentrations of ambient dissolved Fe. For W3 simulations, dissolved Fe was not a limiting factor in recovery efficiency because ambient concentrations were low. The relatively high concentrations of dissolved Fe at sites W4 and W4A (Fig. 15A) never decreased below the SMCL during injection because aquifer sediments contain more reductants such as pyrite and siderite than do sediments at the other sites that buffer the redox conditions; therefore, a lower dissolved Fe concentration of (7.2×10^{-5} M, or 4 mg/L) was substituted at this site and it was named W4B (Fig. 12C). High dissolved Fe concentrations at sites such as these also could result in higher incidences of Fe-related biofouling around the ASR screen; sites with high concentrations of dissolved Fe would probably not be suitable for ASR.

5. Conclusions

ASR technology is under consideration by the New York Department of Environmental Protection for water storage in the unconsolidated deposits that form several important water-supply aquifers beneath Long Island and Staten Island. ASR would be most suitable in Kings, Queens, or Richmond Counties because they are underlain by thick Cretaceous deposits that include the Lloyd aquifer and the Magothy–Jameco aquifer and provide large storage capabilities. ASR has been used on the coastal plain of NJ, including Monmouth County in the northeasternmost part, for many decades.

The deepest Cretaceous aquifer in New York city, the Lloyd aquifer, is confined by a sequence of Cretaceous and Pleistocene confining materials and shows the most promise for potential development. The Cretaceous aquifers in the study area, which include the middle aquifer of the Potomac–Raritan–Magothy (PRM) aquifer system in northeastern NJ, consist of sand and gravel with varying amounts of silt and clay, and contain zones with considerable amounts of lignite and Fe-sulfide minerals.

Core samples from Kings, Queens and Richmond Counties contain high concentrations of Fe, Mn, and acid volatile sulfides (AVS) plus chromium-reducible sulfides (CRS) in some areas, and low concentrations of As, Pb, Cd, Cr, Cu and U. Similarly, water from the Lloyd aquifer in these areas generally contains high concentrations of Fe and Mn and low concentrations of other trace elements, such as As, Pb, Cd, Cr, Cu and U, which were well below USEPA and NY MCLs.

A simplified model of a Cretaceous aquifer such as the Lloyd was used to simulate groundwater- and aquifer-sediment chemistry during a hypothetical 15-a ASR injection and extraction cycle. The model domain was a sand layer 2000 m in length and width and 50 m thick. The reactive-transport simulator, PHAST, was used to simulate ASR at four hypothetical well locations screened in reducing Cretaceous aquifers in western Long Island and northeastern NJ. The simulations entailed injection of oxic NYC drinking water into a hypothetical well for 5a, followed by a 1-a pause, after which groundwater was extracted for 8a. Also, a sensitivity analysis was done, whereby the concentration of pyrite in aquifer sediments was varied (and siderite was added in one simulation), the concentration of buffer in the injectate and the composition of groundwater were varied, in order to represent the uncertainty associated with the spatial variability in aquifer chemistry and the variability in injectate water buffer.

Results were as follows:

1. Injection increased the hydraulic head at the well, displaced the ambient groundwater, and formed a spheroid in the aquifer surrounding the ASR well with lower concentrations of Fe, Mn and major ions than in the ambient water. Injection of buffered water also increased the pe and the pH of water near the well screen.
2. The concentrations of dissolved, exchangeable, and precipitated Fe near the well screen varied with the type of Fe-bearing aquifer mineral, and its reaction under background conditions and in response to ASR injection. The oxidation of Fe^{2+} and subsequent formation of goethite during injection provided a substrate for sorption of dissolved Fe during extraction.
3. The baseline scenario, with a low concentration (0.001 M) of pyrite in aquifer sediments, indicated that about 188% more water can be extracted than was injected without exceeding the SMCL for dissolved Fe of 5.4×10^{-6} M.

4. Extracted water in simulations with high concentrations of pyrite in aquifer sediments generally resulted in less goethite precipitation, greater acidity, and higher concentrations of dissolved Fe than in scenarios with lower pyrite concentrations. The lower pH and smaller amounts of goethite formed during the extraction phase in scenarios with the highest pyrite concentration (0.005 M), decreased the amount of Fe^{2+} sorbed and, therefore, decreased the efficiency of ASR with respect to dissolved Fe concentrations. The scenarios with increased amounts of pyrite in the aquifer resulted in decreased recovery of water with acceptably low concentrations of dissolved Fe (5.4×10^{-6} M). A linear decrease in recovery efficiency is attributed to pyrite dissolution and the associated depletion of DO and increase in acidity. Simulations with more than 0.0037 M of pyrite, which is the maximum amount dissolved in the baseline scenario, had just over a 50% recovery efficiency.
5. The precipitation of ferric hydroxide minerals (goethite) at the well screen, and a possible associated decrease in specific capacity of the ASR well, was not apparent during the extraction phase of the simulations; this could be because the model does not take into account the formation of organic biofilm associated with goethite precipitation on and around the well screen. Goethite dissolution is apparent with the bufferless injectate, and together with the attendant lower pH, indicates that corrosion of the well could be possible.
6. The concentrations of dissolved Fe in extracted water increased with successively decreasing amounts of injectate buffer; this implies that Fe removal could be required after extraction to meet USEPA SMCLs.
7. Differences in the ambient groundwater chemistry affected the chemistry of water extracted from the ASR wells in scenarios in which the injectate was buffered. Dissolved Fe concentrations in extracted water were highest at sites with the highest ambient concentrations of dissolved Fe (sites W4 and W4A).
8. The sensitivity analysis indicated that the greatest impediment to recovery efficiency was high concentrations of pyrite in the aquifer, although concentrations of ambient Fe, and the presence of siderite, also adversely affected recovery efficiency. The addition of a buffer to the injectate increased the recovery efficiency of ASR but to a lesser extent than the amount of the pyrite or ambient dissolved Fe concentrations. Buffering would nevertheless be needed to inhibit corrosion of the well and distribution lines.

Acknowledgements

The New York City Department of Environmental Protection (NYCDEP) provided funding for this project and assistance with drilling and coring.

Appendix A. Supplementary material

Supplementary data associated with this article can be found, in the online version, at doi:10.1016/j.apgeochem.2010.07.001.

References

Appelo, C.A.J., Postma, D., 1993. Geochemistry, Groundwater and Pollution. A.A. Balkema, Rotterdam, Netherlands.
Appelo, C.A.J., Drijverb, B., Hekkenberg, R., de Jonge, M., 1999. Modeling in situ iron removal from groundwater. Ground Water 37, 811–817.
Arbogast, B.F. (Ed.), 1996. Analytical Methods Manual for the Mineral Resource Surveys Program. US Geological Survey. US Geol. Surv. Open-File Rep. 96–525.
Baqai, H.A., 2002. Effects of recharge of chlorinated state water project waters to groundwaters in Lancaster Area of California. Water Eng. Manage. 149 (4), 10–13.
Barksdale, H.C., Greenman, D.W., Lang, S.M., Hilton, G.S., Outlaw, D.E., 1958. Ground-water Resources in the Tri-state Region Adjacent to the Lower Delaware River: New Jersey Department of Conservation and Economic Development, Division of Water Policy and Supply Special Report 13.
Booch, P.W., Barovich, B., 1981. Numerical model describing groundwater treatment by recharge of oxygenated water. Water Resour. Res. 17, 49–56.
Brown, C.J., Schoonen, M.A.A., 2004. Origin of high sulfate concentrations in a coastal plain aquifer. Appl. Geochem. 19, 343–358.
Brown, C.J., Coates, J.D., Schoonen, M.A.A., 1999. Localized sulfate-reducing zones in the Magothy aquifer, Suffolk County, New York. Ground Water 37, 505–516.
Brown, C.J., Rakovan, J., Schoonen, M.A.A., 2000a. Heavy Minerals and Organic Carbon in Pleistocene and Cretaceous sediments on Long Island, with Emphasis on Pyrite and Marcasite in the Magothy Aquifer. US Geol. Surv. Water Resour. Invest. Rep. 99-4216.
Brown, C.J., Schoonen, M.A.A., Candela, J., 2000b. Geochemical modeling of iron, sulfur, oxygen, and carbon in a coastal plain aquifer. J. Hydrol. 237 (3–4), 147–168.
Brown, C.J., Hatfield, K., Newman, M., 2006. Lessons Learned from a Review of 50 ASR Projects from the United States, England, Australia, India, and Africa. US Army Corps of Eng. Rep.
Brown, C.J., Starn, J.J., Stollenwerk, K.G., Mondazzi, R.A., Trombley, T.J., 2009. Aquifer Chemistry and Transport Processes in the Zone of Contribution to a Public-supply Well in Woodbury, Connecticut, 2003–2006. US Geol. Surv. Scient. Invest. Rep. 2009-5051.
Buxton, H.T., Modica, E., 1992. Patterns and rates of ground-water flow on Long Island, New York. Ground Water 30, 857–866.
Buxton, H.T., Shernoff, P.K., 1999. Ground-water Resources of Kings and Queens Counties, Long Island, New York. US Geol. Surv. Water-Supply Paper Rep., p. 2498.
Cartwright, R.A., Chu, Anthony, Candela, J.L., Eagen, V.K., Monti, Jack, Jr., Schubert, C.E., 1998. Ground-water Quality in Kings, Queens, and Western Nassau Counties, Long Island, New York, 1992–1996, with Geophysical Logs from Selected Wells. US Geol. Surv. Open-file Rep. 98-298.
Dempsey, B.A., Roscoe, H.C., Ames, R., Hedin, R., Jeon, B.H., 2001. Ferrous oxidation chemistry in passive abiotic systems for the treatment of mine drainage. Geochem. Explor. Environ. Anal. 1, 81–88.
Dzombak, D.A., Morel, F.M.M., 1990. Surface Complexation Modeling: Hydrous Ferric Oxide. Wiley-Interscience, New York.
Ervin, E.M., Voronin, L.M., Fusillo, T.V., 1994. Water Quality of the Potomac–Raritan–Magothy Aquifer System in the Coastal Plain, West-central New Jersey. US Geol. Surv. Water-resour. Invest. Rep. 94-4113.
Gaus, I., Shand, P., Gale, I., Williams, A., Eastwood, J., 2002. Geochemical modelling of flouride concentration changes during aquifer storage and recovery (ASR) in the Chalk Aquifer in Wessex, England. Quart. J. Eng. Geol. Hydrogeol. 35, 203–208.
Gill, H.E., Farlekas, G.M., 1976. Geohydrologic Maps of the Potomac–Raritan–Magothy Aquifer System in the New Jersey Coastal Plain. US Geol. Surv. Atlas HA-557, 2 Sheets, Scale 1:500,000.
Hallberg, R., Martinell, R., 1976. Vyredox – in situ purification of groundwater. Ground Water 14, 88–93.
Hsieh, P.A., Winston, R.B., 2002. User's Guide to Model Viewer, a Program for Three-dimensional Visualization of Ground-water Model Results. US Geol. Surv. Open-File Rep. 02-106.
Jensen, D.L., Boddum, J.K., Tjell, J.C., Christensen, T.H., 2002. The solubility of rhodochrosite ($MnCO_3$) and siderite ($FeCO_3$) in anaerobic aquatic environments. Appl. Geochem. 17, 503–511.
Katzer, T., Brothers, K., 1989. Artificial recharge in Las Vegas Valley, Clark County, Nevada. Ground water 27, 50–56.
Knobel, L.L., Chapelle, F.H., Meisler, H., 1998. Geochemistry of the Northern Atlantic Coastal Plain aquifer system. US Geol. Surv. Prof. Paper 1404-L.
Lacombe, P.J., 1996. Artificial Recharge of Ground Water by Well Injection for Storage and Recovery, Cape May County, New Jersey, 1958–1992 (SuDoc I 19.76:96-313).
Lani, M., Schoonen, M.A.A., 1996. The Influence of Cation Exchange on the Chemistry of Long Island Groundwater. In: Geology of Long Island and Metropolitan New York. Long Island Geologists, Stony Brook, NY, pp. 104–109.
Lovley, D.R., 1987. Organic matter mineralization with the reduction of ferric iron—a review. Geomicrobiol. J. 5, 375–399.
Lovley, D.R., Phillips, E.J.P., 1987. Rapid assay for microbially reducible ferric iron in aquatic sediments. Appl. Environ. Microbiol. 53, 1536–1540.
Lovley, D.R., Coates, J.D., Blunt-Harris, E.L., Phillips, E.J.P., Woodward, J.C., 1996. Humic substances as electron acceptors for microbial respiration. Nature 382, 445–448.
Luzier, J.E., 1980. Digital Simulation and Projection of Head Changes in the Potomac–Raritan–Magothy Aquifer System, Coastal Plain, New Jersey. US Geol. Surv. Water Resour. Invest. Rep. 80-11.
McKibben, M.A., Barnes, H.L., 1986. Oxidation of pyrite in low temperature acidic solutions—rate laws and surface textures. Geochim. Cosmochim. Acta 50, 1509–1520.
Mettler, S., Abdelmoula, M., Hoehn, E., Schoenenberger, R., Weidler, P., von Gunten, U., 2001. Characterization of iron and manganese precipitates from an in situ groundwater treatment plant. Ground Water 39, 921–930.
Mirecki, J.E., 2004. Water-quality Changes During Cycle Tests at Aquifer Storage Recovery (ASR) Systems in South Florida. US Army Corps of Engineers, Engineer Research and Development Center, TR-04-8.

Misut, P.E., Voss, C.I., 2007. Freshwater-saltwater transition zone movement during aquifer storage and recovery cycles in Brooklyn and Queens, New York City, USA. J. Hydrol. 337, 87–103.

Moses, C.O., Nordstrom, D.K., Herman, J.S., Mills, A.L., 1987. Aqueous pyrite oxidation by dissolved oxygen and ferric iron. Geochim. Cosmochim. Acta 51, 1561–1571.

Murowchick, J.B., Barnes, H.L., 1986. Marcasite precipitation from hydrothermal solutions. Geochim. Cosmochim. Acta 50, 2615–2630.

Nordstrom, D.K., 1982. Aqueous pyrite oxidation and the consequent formation of secondary iron minerals. In: Kittrick, J.A., Fanning, D.S., Hossner, L.R., Kral, D.M., Sherri, H. (Eds.), Acid Sulfate Weathering. Proc. Symp. Soil Science Society of America. SSSA Special Publication 10, Madison, WI, pp. 37–56.

New York City Department of Environmental Protection (NYCDEP), 2002. Underground Water Storage and Water Supply Pilot-test Work Plan—Brooklyn Queens Aquifer Feasibility Study. Jamaica, New York.

Parkhurst, D.L., Appelo, C.A.J., 1999. User's Guide to PHREEQC (version 2)—A Computer Program for Speciation, Reaction-path, 1D Transport, and Inverse Geochemical Calculations. US Geol. Surv. Water-resour. Invest. Rep. 99-4259.

Parkhurst, D.L., Kipp, K.L., Engesgaard, P., Charlton, S.R., 2004. PHAST – A Program for Simulating Ground-water Flow, Solute Transport, and Multicomponent Geochemical Reactions. US Geol. Surv. Tech. and Methods 6-A8.

Pavelic, P., Dillon, P.J., 1997. Review of International Experience in Injecting Natural and Reclaimed Waters into Aquifers for Storage and Reuse. Centre for Groundwater Studies Rep. No. 74 (May 1997).

Pavelic, P., Dillon, P.J., Barry, K.E., Vanderzalm, J.L., Correll, R.L., Rinck-Pfeiffer, S.M., 2007. Water quality effects on clogging rates during reclaimed water ASR in a carbonate aquifer. J. Hydrol. 334, 1–16.

Pearson Jr., F.J., Friedman, I., 1970. Sources of dissolved carbonate in an aquifer free of carbonate minerals. Water Resour. Res. 6, 1775–1781.

Perlmutter, N.M., Arnow, T., 1953. Ground Water in Bronx, New York, and Richmond Counties with Summary Data on Kings and Queens Counties, New York City, New York. New York State Water Power and Control Commission Bulletin GW-32.

Postma, D., 1982. Pyrite and siderite formation in brackish and freshwater swamp sediments. Am. J. Sci. 282, 1151–1183.

Pucci Jr., A.A., Ehlke, T.A., Owens, J.P., 1992. Confining effects of groundwater quality in the New Jersey Coastal Plain. Ground Water 30, 415–427.

Pucci, A.A., Jr., Pope, D.A., Gronberg, J.M., 1994. Hydrogeology, Simulation of Regional Groundwater Flow, and Saltwater Intrusion, Potomac–Raritan–Magothy Aquifer System, Northern Coastal Plain of New Jersey. New Jersey Geol. Surv. Rep. 36.

Pyne, R.D.G., 1995. Groundwater Recharge and Wells: A Guide to Aquifer Storage Recovery. Lewis Publishers, Boca Raton, Florida.

Rott, U., Lamberth, B., 1993. Groundwater cleanup by in situ treatment of nitrate, iron and manganese. Water Supply 11, 143–156.

Singer, P.C., Stumm, W., 1970. The solubility of ferrous Iron in carbonate-bearing waters. J. Am. Water Works Assoc. 62, 198–202.

Smolensky, D.A., Buxton, H.T., Shernoff, P.K., 1989. Hydrologic Framework of Long Island, New York. US Geol. Surv. Hydrol. Invest. Atlas HA-709.

Soren, J., 1988. Geologic and Geohydrologic Reconnaissance of Staten Island, New York. US Geol. Surv. Water-resour. Invest. Rep. 87-4048.

US Environmental Protection Agency (USEPA), 2008. Title 40—Protection of Environment, Chapter I Environmental Protection Agency, Part 141—National Primary Drinking Water Regulations. Washington, DC. <http://www.epa.gov/safewater/contaminants/index.html#primary>. (accessed 20.10.09.).

Vacher, H.L., Hutchings, W.C., Budd, D.A., 2006. Metaphors and models: the ASR bubble in the Floridan Aquifer. Ground Water 44, 144–154.

Van Beek, C.G.E.M., 1980. A Model for the Induced Removal of Iron and Manganese from Groundwater in the Aquifer. In: Proc. 3rd Water-Rock Interaction Symp., Edmonton, Canada, pp. 29–31.

Van Beek, C.G.E.M., Vaessen, H., 1979. In situ iron removal from groundwater. H_2O, 12, 15–19 (in Dutch).

Walter, D.A., 1997. Effects and Distribution of Iron-related Well-screen Encrustation and Aquifer Biofouling in Suffolk County, Long Island, New York. US Geol., Surv., Water-resour. Invest. Rep. 96-4217.

Zapecza, O.S., 1989, Hydrogeologic Framework of the New Jersey Coastal Plain. US Geol. Surv. Prof. Paper 1404-B.